

# FUSION REACTIONS AND MATTER-ANTIMATTER ANNIHILATION FOR SPACE PROPULSION

**Claude DEUTSCH**

*LPGP (UMR-CNRS 8578), Bât. 210, UPS, 91405 Orsay, France*

**RÉSUMÉ** : La fusion par confinement magnétique (FCM) et la fusion par confinement inertiel (FCI) sont comparées dans le contexte de missions à longue distance, à travers le système solaire. Ces deux approches montrent des capacités manœuvrières bien supérieures, à celles de la propulsion cryogénique standard (PCS). Les contraintes de coût sont bien inférieures à celles exigées par la production d'énergie, au sol. Un problème crucial est celui du décollage (problématique des 300 premiers kms), étant donné les risques de pollution radioactive de la basse atmosphère. Il est recommandé d'assembler le vaisseau spatial à haute altitude  $\sim 700$  kms, ou mieux, sur la lune. En ce qui concerne les impulsions spécifiques en sec, on s'attend à 500-3000 pour la fission, et jusqu'à  $10^4$ - $10^5$  pour la fusion deuterium + tritium.

Enfin, on aborde la réaction de fusion la plus performante, l'annihilation  $p$ - $\bar{p}$  avec  $I_{sp}$  (sec)  $\sim 10^3$ - $10^6$  et un rapport poussée/poids  $\sim 10^{-3}$ -1. Production et coûts sont détaillés, autant que possible. Ces derniers pourraient être réduits de quatre ordres de grandeur, si la fusion contrôlée devenait économiquement viable.

On discute plusieurs schémas de propulsion par annihilation matière-antimatière. On accorde une certaine attention à la propulsion par fusion inertielle et catalysée par annihilation de  $\bar{p}$ , et en particulier, au projet ICAN-II, potentiellement en mesure d'atteindre Mars en 30 jours en utilisant une fusion catalysée par 140 ng de  $\bar{p}$  avec une impulsion spécifique  $\sim 13500$  sec.

**ABSTRACT**: Magnetic confinement fusion (MCF) and inertial confinement fusion (ICF) are critically contrasted in the context of far-distant travels throughout solar system.

Both are shown to potentially display superior capabilities for vessel maneuvering at high speed, which are unmatched by standard cryogenic propulsion (SCP).

Costs constraints seem less demanding than for ground-based power plants. Main issue is the highly problematic takeoff from earth, in view of safety hazards concomitant to radioactive spills in case of emergency. So, it is recommended to assemble the given powered vessel at high earth altitude  $\sim 700$  km, above upper atmosphere.

Report Documentation Page				Form Approved OMB No. 0704-0188	
Public reporting burden for the collection of information is estimated to average 1 hour per response, including the time for reviewing instructions, searching existing data sources, gathering and maintaining the data needed, and completing and reviewing the collection of information. Send comments regarding this burden estimate or any other aspect of this collection of information, including suggestions for reducing this burden, to Washington Headquarters Services, Directorate for Information Operations and Reports, 1215 Jefferson Davis Highway, Suite 1204, Arlington VA 22202-4302. Respondents should be aware that notwithstanding any other provision of law, no person shall be subject to a penalty for failing to comply with a collection of information if it does not display a currently valid OMB control number.					
1. REPORT DATE <b>13 JUL 2005</b>		2. REPORT TYPE <b>N/A</b>		3. DATES COVERED <b>-</b>	
4. TITLE AND SUBTITLE <b>řFusion Reactions And Matter-Antimatter Annihilation For Space Propulsion</b>				5a. CONTRACT NUMBER	
				5b. GRANT NUMBER	
				5c. PROGRAM ELEMENT NUMBER	
6. AUTHOR(S)				5d. PROJECT NUMBER	
				5e. TASK NUMBER	
				5f. WORK UNIT NUMBER	
7. PERFORMING ORGANIZATION NAME(S) AND ADDRESS(ES) <b>LPGP (UMR-CNRS 8578), Bât. 210, UPS, 91405 Orsay, France</b>				8. PERFORMING ORGANIZATION REPORT NUMBER	
9. SPONSORING/MONITORING AGENCY NAME(S) AND ADDRESS(ES)				10. SPONSOR/MONITOR'S ACRONYM(S)	
				11. SPONSOR/MONITOR'S REPORT NUMBER(S)	
12. DISTRIBUTION/AVAILABILITY STATEMENT <b>Approved for public release, distribution unlimited</b>					
13. SUPPLEMENTARY NOTES <b>See also ADM001791, Potentially Disruptive Technologies and Their Impact in Space Programs Held in Marseille, France on 4-6 July 2005.</b>					
14. ABSTRACT					
15. SUBJECT TERMS					
16. SECURITY CLASSIFICATION OF:			17. LIMITATION OF ABSTRACT <b>UU</b>	18. NUMBER OF PAGES <b>41</b>	19a. NAME OF RESPONSIBLE PERSON
a. REPORT <b>unclassified</b>	b. ABSTRACT <b>unclassified</b>	c. THIS PAGE <b>unclassified</b>			

Fusion propulsion is also compared to fission powered one, which secures a factor of two improvement over SCP.

As far a specific impulse (sec) is considered, one expects 500-3000 from fission and as much as  $10^4 - 10^5$  from fusion through deuterium-tritium. Next, we turn attention to the most performing fusion reaction, i.e. proton-antiproton annihilation with specific impulse  $\sim 10^3 - 10^6$  and thrust-to-weight ratio  $\sim 10^{-3} - 1$ . Production and costs are timely reviewed. The latter could drop by 4 orders of magnitude, which is possible with successful MCF or ICF.

Appropriate vessel designs will be presented for fusion as well as for antimatter propulsion. In particular, ICAN-II project to Mars in 30 days with fusion catalyzed by 140 ng of antiprotons will be detailed (specific impulse  $\sim 13500$  sec).

## I - INTRODUCTION - IMPOSSIBLE MISSIONS

There are missions in the solar system that would be desirable to accomplish for scientific purposes, but which are essentially impossible using chemical or even nuclear thermal rockets. One example is a solar impact mission, which requires the rocket to cancel out the orbital velocity of the earth so the vehicle can drop directly into the sun. This requires a mission characteristic velocity of 35 km/s, which is presently obtained by an out-of-the-way swingby of Jupiter, 5 AU and many years in the wrong direction. Another is a mission to the rings deep down in the gravity well of Saturn. This requires a mission characteristic velocity of 48 km/s.

There are even much simpler missions near earth that are nearly impossible using chemical rockets. One is the simple maneuver of rapidly reversing your orbital direction. This maneuver requires cancelling the initial orbital velocity and building it up again in the opposite direction. Since earth orbital velocity is 7.7 km/s, the total mission characteristic velocity of the reverse orbit maneuver is 15.5 km/s. If it is then desired to return to the initial orbit (to dock at an orbiting space station base), the process must be repeated with a total mission characteristic velocity of 31 km/s [1].

The mass ratios required for each type of rocket system to carry out each of these missions can be calculated from the rocket equation

$$R = \frac{m_v + m_p}{m_v} = e^{\Delta V / v_{ex}} = e^{\Delta V / g I_{sp}} \quad , \quad [1.]$$

in terms of requested velocity variations  $\Delta V$ , where  $m_v$  is the mass of the empty vehicle (including payload) delivered to destination and  $m_p$  denotes propellant mass exhausted at velocity  $V_{ex}$  or specific impulse  $I_{sp}$  while  $g = 9.8 \text{ m/s}^2$  is gravitation constant at earth surface.

Above discussed mass ratio are listed in table I. As can be seen, all of these mission require high mass ratios, with the more difficult ones requiring such large mass ratios that it is difficult, if not impossible, to imagine how one might build a vehicle to accomplish those missions using chemical or nuclear thermal rockets. All of those missions could be performed by fusion or antimatter rockets with a mass ratio of 5:1 or less.

Table I - Mass ratios for difficult missions

		Total mass ratio		
		Storable	H <sub>2</sub> /O <sub>2</sub>	Nuclear
	I <sub>sp</sub> =	300 s	500 s	900 s
	$\Delta v$ (km/s)			
Reverse orbit	15,5	175	22	6
Double reverse orbit	31	30,700	490	32
Solar impact	35	117,000	1,100	49
Saturn ring rendezvous	48	8,900,000	15,000	200

In this connection, it is appropriate to recall that nuclear (fission) thermal propulsion could provide only a factor of two improvement upon standard cryogenic propulsion (SCP).

Viewing matter annihilation as the upper limit of what thermonuclear propulsion can achieve, we denote our present analysis to the various approaches affordable through fusion in a broad sense for long distance journeys throughout the solar system. Fusion thus indeed appears as the only option that potentially achieves the most important regime for solar system travel:

— Exhaust velocities of  $10^5$  to  $10^6$  m/s at thrust-to-weight ratio of  $10^{-3}$ . Such levels of performance allow both human and efficient cargo transport. Specific parameters qualifying various propellants are detailed on Table II

Table II - Propellant parameters

Propulsion type	Specific impulse [sec]	Thrust-to-weight Ratio
Chemical bipropellant	200 - 410	.1 - 10
Electromagnetic	1200 - 5000	$10^{-4}$ - $10^{-3}$
Nuclear fission	500 - 3000	.01 - 10
Nuclear Fusion	$10^4$ - $10^5$	$10^{-5}$ - $10^{-2}$
Antimatter annihilation	$10^3$ - $10^6$	$10^{-3}$ - 1

It is highly suggestive to notice that 100 mg of antimatter are equivalent to the space shuttle propulsive energy.

## 2 - BASIC CONCEPTS

The potential benefits of space propulsion by nuclear fusion will be briefly motivated here by a simple analysis.

Roughly, to accelerate a mass  $M_w$  to a speed  $v_c$  in a time  $\tau$  requires a thrust power  $P_w$  given by

$$P_w = (\frac{1}{2} M_w v_c^2) / \tau \quad , \quad [2.]$$

from which we define the characteristic velocity  $v_c$  by

$$v_c = (2\alpha\tau)^{1/2} \quad . \quad [3.]$$

Here  $\alpha = P_w/M_w$  is the specific power, defined in relation to the mass  $M_w$  of the propulsion system. The corresponding flight distance  $L$  is roughly related to the flight time by

$$\tau = K_0 L/v_c \quad , \quad [4.]$$

where  $K_0$  is a constant of order unity. Combining Eqs. (2)-(4) gives, with appropriate units conversions, yields

$$\tau(\text{years}) = 0.2 \frac{[L(\text{astronomical units})]^{2/3}}{[\alpha(\text{kW/kg})]^{1/3}} \quad . \quad [5.]$$

Here we have chosen  $K_0 = 3$  to provide a reasonable fit to example orbit calculations in the literature.

The payload delivered is the other key figure of merit besides the flight time in assessing rocket performance. The payload mass (including rocket structure) can be related to the initial rocket mass, including propellant, by the well-know rocket Eq. 1.

Optimum payload management typically corresponds to  $v_c = \sqrt{2} v_{ex}$ , with a final velocity near the characteristic velocity. Thus, to reach 1 A.U. in 1 year with a 0.1 payload fraction at a specific power of 1 kW/kg requires an exhaust velocity on the order of  $10^5$  m/s, or a specific impulse of about  $10^4$  s. These parameters are consistent with a magnetic fusion dipole fusion rocket [2], but are beyond the capabilities of either nuclear fission thermal systems, in which reactors heat the propellant directly (high specific power, but lower specific impulse), or nuclear fission electric systems, in which reactors supply electricity to ion accelerators (high specific impulse, but low power).

Figure 1 plots Eq. 5 for various high specific impulse systems and illustrates the potential of fusion propulsion. All values plotted in Fig. 1 correspond to  $v_{ex} < 10^6$  ms<sup>-1</sup>, well within the capability of fusion rockets. In a fusion rocket  $v_{ex}$  can be readily adjusted up to  $v_{ex} \cong 10^7$  ms<sup>-1</sup> or a specific impulse of  $10^6$  s, corresponding to direct exhaust of the hot fuel as propellant, and even faster speeds could be achieved by selective exhaust of certain reaction products. However, as already noted, specific power rather than specific impulse is the primary constraint.

Specific powers in the range of 1 kW/kg, already an order of magnitude better than nuclear fission electric systems, appear quite feasible, and we shall discuss one such system, the dipole. As one can see from the figure, at a few kW/kg specific power, interplanetary trips would require only months, and the Tau mission (thousand astronomical units) would require only 10-20 years.

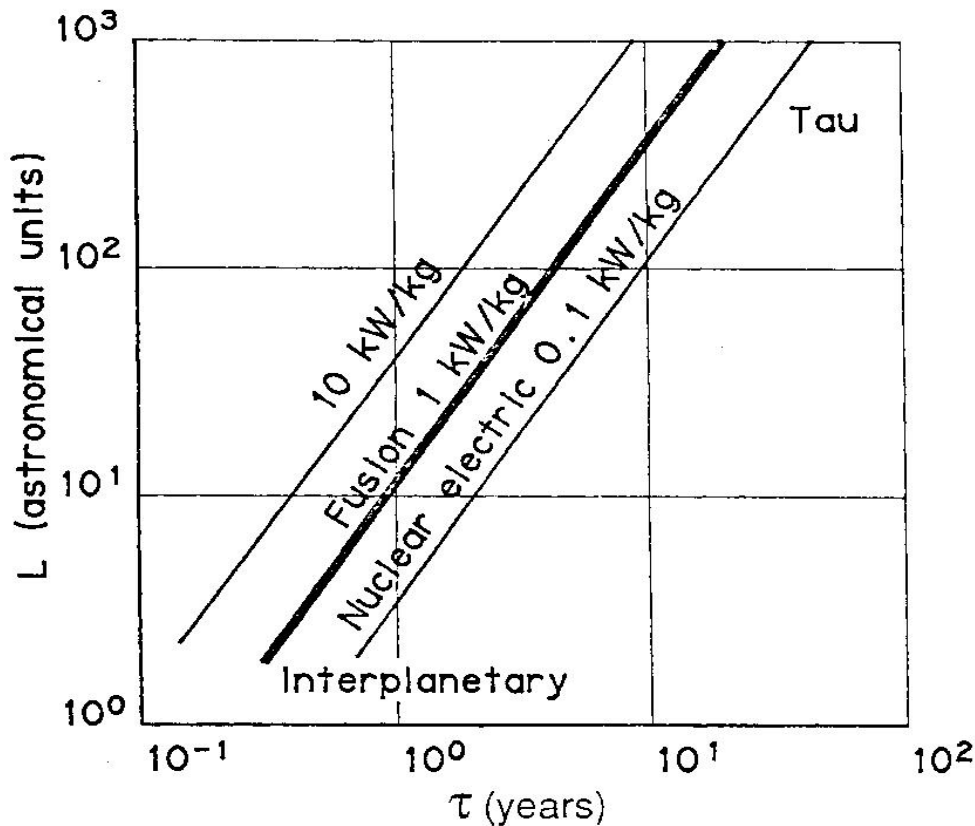


**Figure 1** - Mission distance  $L$  versus flight time  $\tau$  for different ratios of thrust power to mass of propulsion system.

### 3 - ENVIRONMENTAL HAZARDS [3]

#### 3.1 - HAZARDS IN EARTH MAGNETOSPHERE

Apollo astronauts (moon mission) received 50 rads  $\sim$  10% lethal dose L-50. Secure manipulations on low orbits (300-500 kms) are mandatory. Trapped particles in magnetosphere are mostly hydrogen ( $\sim$  olympic pool).

Propellant quantity (ergol) needed for interplanetary missions at  $I_{sp}$  maximum  $\sim$  quantity of trapped matter.

Unused fuel and propellant can pollute magnetosphere, when electrically charged, these residues can be magnetically trapped and lifted down in the atmosphere. Radioactive fuel, moderator or shield material can be found in earth gravitation field, when a Columbia type hazard takes places  $\rightarrow$  earth surface.

Once activated, fission or fusion reactors should be parked on a high orbit ( $\sim$  700 kms). Magnetosphere orbits lie above LEO (low Earth Orbits). Bonus for reactors with short radioactive periods.

#### 3.2 - TRITIUM IN SPACE

Tritium is biologically active, about 9600 Ci/gram, and must not be released in the atmosphere.

5 kilograms of tritium is about equivalent, in Curies, to the biologically active Chernobyl release. Its biological hazard potential, however, is much less.

Because of mass limitations, DT reactors in space would probably not be able to support a blanket to breed tritium, or recover tritium from the escaping plasma of a direct fusion rocket.

The fuel burn-up fraction for magnetic DT reactors is likely to lie between  $0.05 < F < 0.20$ . Thus, from 5 to 20 times as much tritium fuel will be needed as is actually burned.

A 200 MWT DT reactor, characteristic of direct fusion rockets, will need from 1 to 4 kilograms of tritium per day to operate.

### 3.3 - ACCIDENTS

If a year's tritium supply were carried aboard a single shuttle flight, the potential release in Curies (but not in biological hazard potential) would be 73 to 292 times that of Chernobyl.

The relative hazards of the radioactive inventories of fission and fusion reactors parked in a nuclear safe orbit can be assessed by comparing the 1 GwE Chernobyl fission reactor to the 1 GwE Starfire DT fusion reactor study, the radioactive inventory of which was estimated at the end of one year of operation.

#### The Chernobyl accident:

- λ Released into the environment about 50 MCi of noble gases.
- λ Released into the environment about 50 MCi of additional biologically active fission products.
- λ Had a core inventory of about 1500-2000 MCi at the time of the accident.

#### 3.3.1 - Accident Scenarii

Figure 2 highlights many hazards likely to occur from the use of fusion propulsion in the vicinity of the earth atmosphere and magnetosphere. Elaborating on recent space events, one is led to the following classification:

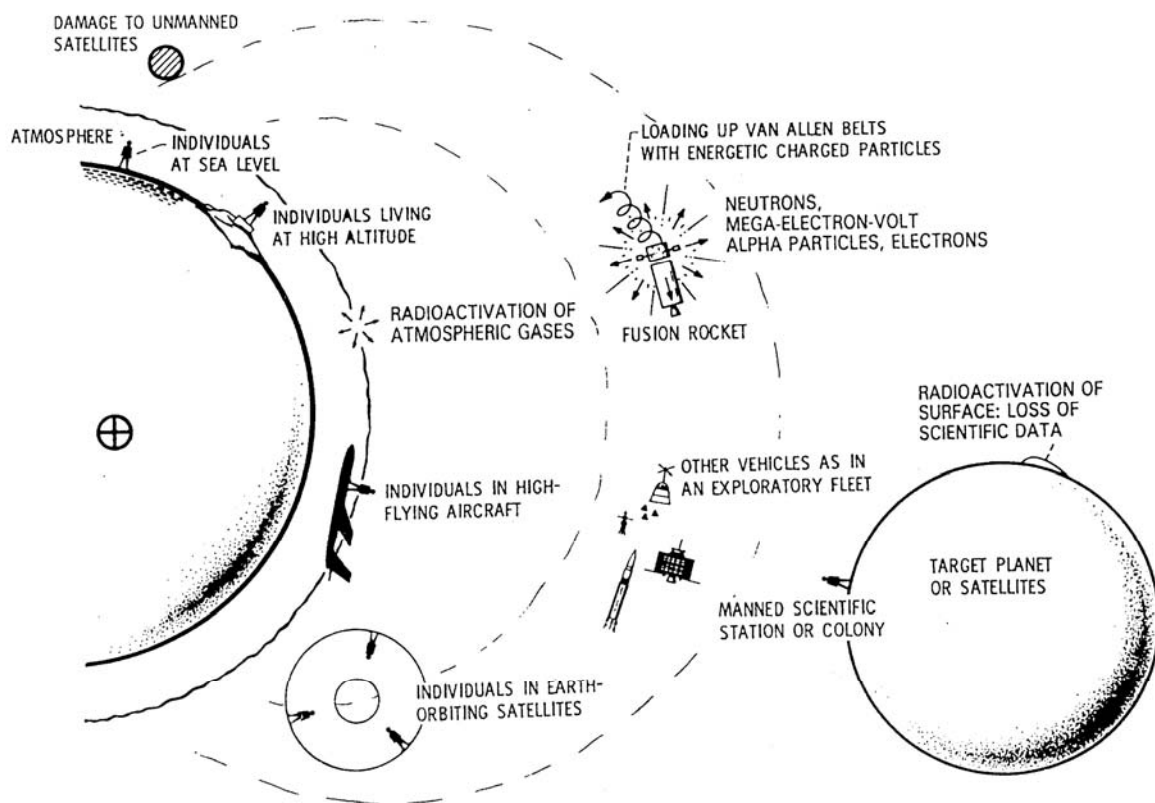


Figure 2 - Potential environmental hazards of fusion propulsion system (after Reece Rothe [3])

a)- Challenger-type accident on way to orbit:

Fission systems: Relatively inconsequential - reactor inert and not yet activated.

Fusion systems: Potentially serious if tritium inventory is released into the atmosphere or magnetosphere.

b)- Columbia-style re-entry of structure and fuel inventory:

Fission systems: Grave fallout hazard from fission products and activated structure.

Fusion systems: Fallout hazard from structure and tritium inventory.

c)- Leakage of unburned fuel in exhaust:

Fission systems; Relatively small hazard.

Fusion systems: Fallout hazard of tritium in the atmosphere or magnetosphere.

Then, comparing several fusion reactions (Table III) one can witness through an evaluation of safety distance from neutron production, that  $D^3He$  reaction is much more fitted to space propulsion than the usual DT, when safety concerns are taken care of.

Table III - Safe distance from unshielded fusion reactor with isotropic neutron production

Fusion reaction	Neutron fraction	Neutron energy E, MeV	Safe distance $R_1$ , KM	$R_1/R_0$ , in earth RADII
DT	0.80	14.07	16,800	2.6
DD	0.336	2.45	14,300	2.2
cat. DD	0.38	8.26	8,600	1.4
$D^3He$	0.02	2.45	2,900	0.45
$p^6Li$	0.05	1.75	5,500	0.86

**Assumptions:**

a)- 200 MW of charged particle power.

b)- Safe dose for continuous exposure to MeV neutrons: 10 neutrons/cm<sup>2</sup> - sec.

c)- Earth radius  $R_0 = 6,378$  km.

### 3.4-D- $^3He$ FUEL IS MORE ATTRACTIVE FOR SPACE APPLICATIONS THAN D-T FUEL

λ High charged-particle fraction allows efficient direct conversion of fusion power to thrust of electricity.

◇ Increases useful power.

◇ Reduces heat rejection (radiator) mass.

◇ Allows flexible thrust and exhaust velocity tailoring.



- λ Low neutron fraction reduces radiation shielding.
- λ  $D-^3He$  eliminates the need for a complicated tritium-breeding blanket and tritium-processing system.

#### 4 - MAGNETIC FUSION ENERGY (MFE)

When more than a few hundred kilowatts of steady-state power are required for space applications, the only feasible choices appear to be nuclear fission or nuclear fusion. Space application places different and usually more stringent constraints on the choice of fusion reactions and fusion confinement systems than do ground-based electric utility applications. In space, the dominant constraint is a minimum mass per unit of power output; for ground-based utilities, the cost of electricity is the dominant constraint. Forseeable applications of fusion reactors to space-related power and propulsion systems appear to require thermal power levels ranging from 10 MW up to 1 GW. There appears to be no mission for the multigigawatt reactors currently of interest to the electrical utilities. Desirable characteristics of fusion reactors for space include avoidance of tritium-fueled reactions; and operation that is as nearly aneutronic as possible; a steady-state operation; an operation at high beta, with a plasma stability index greater than  $\beta = 0.20$ ; the use of direct conversion or direct production of thrust to minimize the power flows that must be handled by heavy energy conversion equipment; and a value of the system-specific mass below  $\alpha = 5 \text{ kg/KW}$  (electric), to be competitive with fission systems for space applications. Only the deuterium-tritium reaction appears feasible for magnetic fusion reactors having large recirculating power flows; for reactors with little recirculating power, the best all-around fusion reaction for space applications appears to be  $D^3He$ .

##### 4.1 - $D-^3He$

A preliminary assessment of propulsion with  $D^3He$  fusion is given on Figure 3, where specific impulse is evaluated for several propellants.

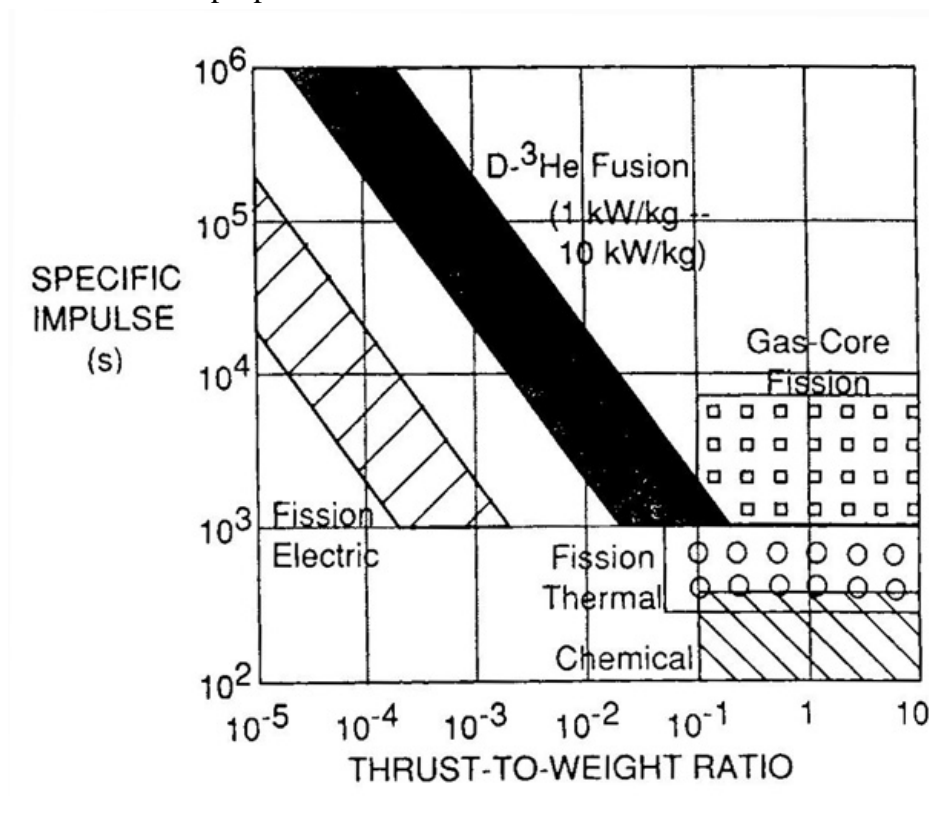


**Figure 3** - Comparison of D-<sup>3</sup>He fusion with chemical, nuclear thermal, and nuclear electric propulsion systems.

### Advantages of D-<sup>3</sup>He magnetic fusion for space applications

- λ No radioactive materials are present at launch, and only low-level radioactivity remains after operation.
- λ Conceptual designs project higher specific power values (1-10 kW-thrust/kg) for fusion than for nuclear-electric or solar-electric propulsion.
- λ Fusion gives high, flexible specific impulses (exhaust velocities), enabling efficient long-range transportation.
- λ D-<sup>3</sup>He produces net energy and is available throughout the Solar System.
- λ D-<sup>3</sup>He fuel provides an extremely high energy density.

## 4.2 - TOROIDAL SYSTEMS

Among systems implementing thermonuclear fusion through magnetic confinement, the tokamak architecture is far a head by virtue of superior performance in the laboratory. A typical propulsion scenario using the given toroidal geometry is depicted on Figure 4.

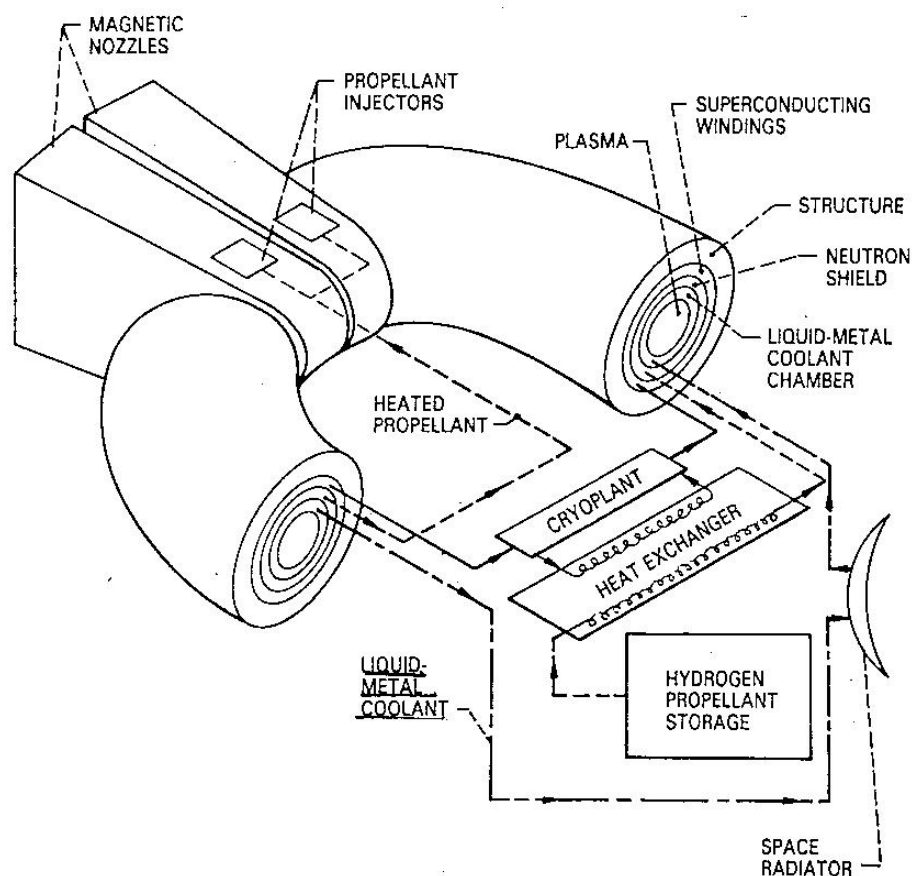


**Figure 4** - Major subsystems of toroidal fusion rocket propulsion system [3]

However, space applications appear to favor other configurations such as the dipole discussed below [2]. The main reason is the need for simplicity and high specific power, always advantageous but absolutely necessary for space propulsion. Because the tokamak requires a strong toroidal field

provided by massive coils interlinking the plasma, it will likely be difficult for tokamak designs to meet the specific power requirements outlined in Section II. Also, again because of the strong toroidal magnetic field, in the tokamak as normally configured there is no path of escape for the hot propellant plasma (as is required to produce thrust directly), and providing such an escape path would require a magnetic divertor far more massive and complex than the usual tokamak divertor that only serves to dump heat inside the machine.

Among the magnetic confinement systems that may in principle be better suited to space propulsion are the open systems as schematized on Figure 5, in which magnetic lines leaving the open ends of the machine provide a natural divertor. The best-studied open system is the tandem mirror. A detailed study of the tandem mirror for space applications yielded a specific power around 1 kW/kg, in the range of interest as discussed in Section II.

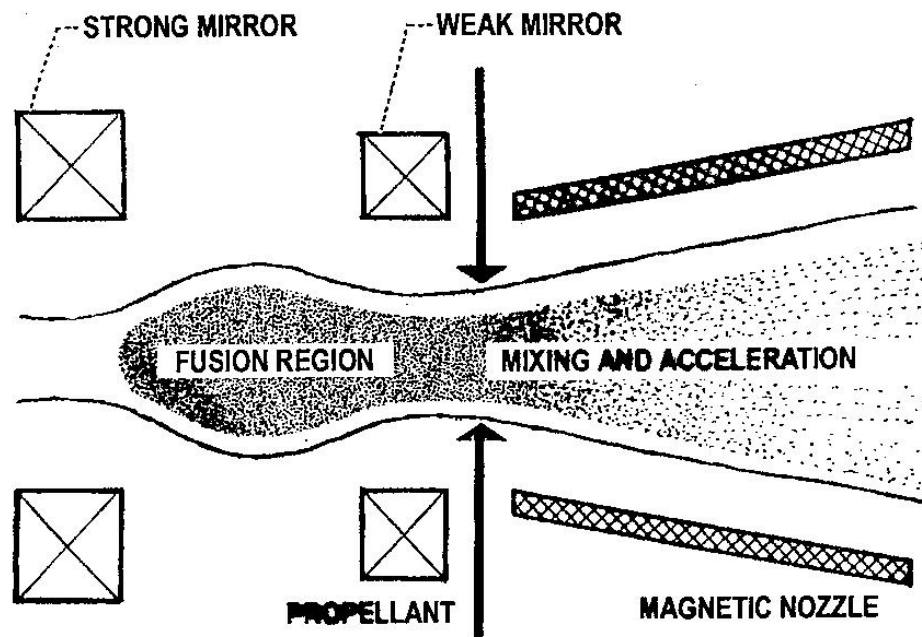


**Figure 5** - System for direct production of thrust from open magnetic configuration

### 4.3 - MAGNETIC DIPOLE

Here we have chosen as a different example the magnetic dipole configuration which, though less well studied than tokamaks and tandem mirrors, appears to offer advantages in terms of mass and simplicity. As in the tandem mirror study cited above, here we also consider the D-<sup>3</sup>He nuclear fusion process. We choose this process over the more conventional D-T fusion reaction because mainly charged particles are produced, the only neutrons being those from secondary D-D reactions and tritium produced by these reactions. Producing fewer neutrons requires less massive shielding and less massive radiators to dispose of waste heat (the only way to do so in space). The predominantly charged-particle energy output allows thrust to be produced directly by the plasma exhaust without recourse to inefficient conversion of heat to electricity to drive ion engines. Also, it is known that, through eons of solar-wind deposition, <sup>3</sup>He is abundantly available on the moon [4].

The dipole, being somewhat simpler than the tokamak or the tandem mirror, is expected to be less massive than either of these devices at the same power, and therefore the dipole may produce greater specific power. The overall configuration is shown in Fig. 6, Coil C (the dipole) carries a large

current, of order 50 MA, and provides the strong field that confines the D-<sup>3</sup>He plasma in an annulus about the coil.

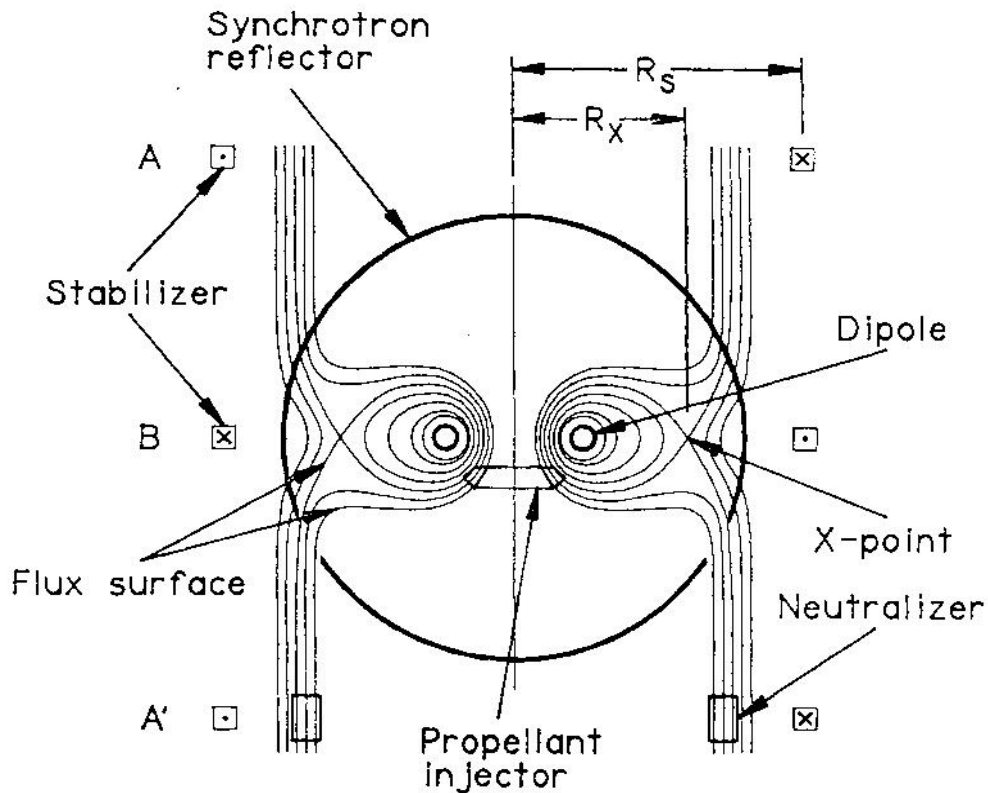


**Figure 6** - Dipole reactor propulsion scheme (Teller *et al.* [2])

Coils A, A', and B (the stabilizer) provide a weaker field that levitates the dipole against gravity or acceleration, at a stable position between the coils. The stabilizer also serves as the "divertor", whereby the closed magnetic lines of the dipole open up beyond the so-called separatrix flux surface containing an X-point (field null). Heat diffusing onto the open lines provides the power to create thrust in the form of a magnetically accelerated ion beam that is converted to neutral atoms as it exits the rocket. This means of converting the energy of the magnetically confined plasma to a directed neutral beam is similar in principle to the neutral beam injectors now being used to heat tokamaks. The arrangement to accomplish this, is sketched in Fig. 7.

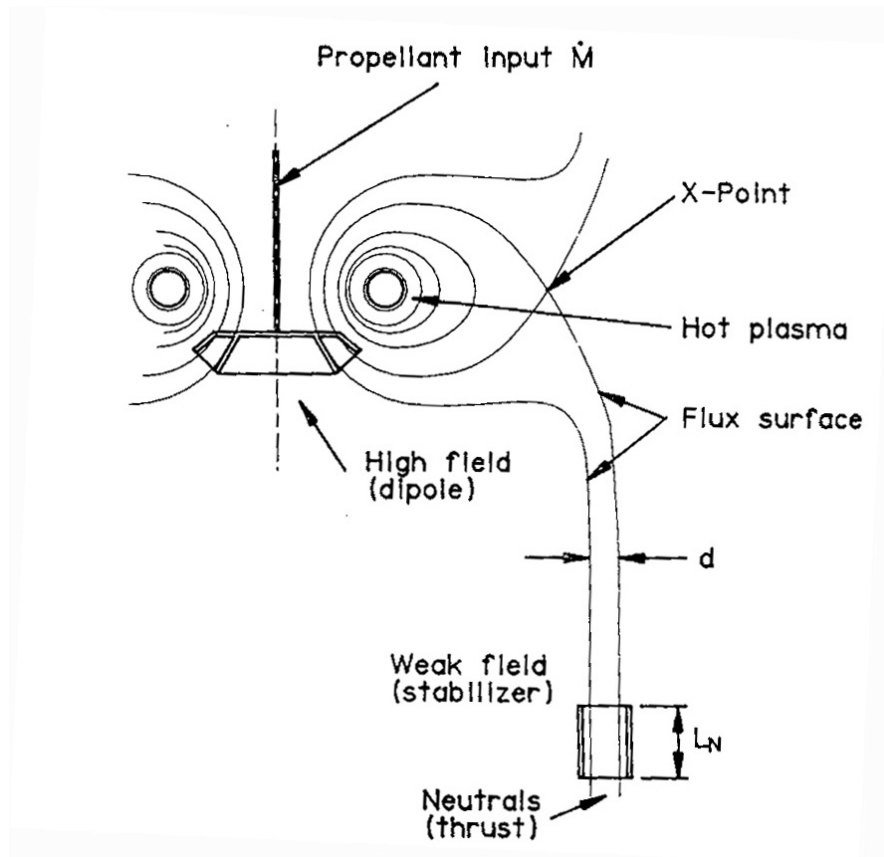


**Figure 7** - Detail of propellant feed and thruster ([2])

#### 4.4 - IMPLEMENTATION

For the contemplated missions for space travel, especially those of long duration, long-term operation with minimum maintenance is particularly important. The proposed dipole configuration is attractive for this application, because it involves no moving parts except those needed for fuel injection and internal refrigeration. Sample parameters shown in Table IV suggest that specific powers of 1 kW/kg, at a specific impulse of up to  $3 \times 10^5$  s are possible. The relatively open structure of the dipole should simplify in-flight maintenance, which will rely on extensive use of robotics. Extensive experimentation is required, however, to assess the feasibility of long-term expeditions, and to minimize cost.

Although the dipole is fundamentally a simple structure, detailed consideration must be given to the design and construction of ancillary systems such as the internal cooling system for the central conductor, the fuel system, the support coils, and the neutralizer. The ultimate performance of the system will be very sensitive to the efficiency of the neutralizer, and to the directionality of the output flow.

Maintenance and reliability are issues of paramount importance for deep space missions. For example, it may be necessary to develop the technology to segment the superconducting ring, to facilitate its repair in flight. Techniques for initiating the fusion burn in the dipole configuration and for restarting it in mid-mission must also be developed.

A further problem is the continued operation of automatic equipment for making measurements and for appropriate communication. This must be accomplished by apparatus that can survive operation in a high flux of energetic neutrons. The flux can be minimized by shielding or by distance, but a practical and optimal solution to this problem requires explicit proof.

Most of the physics research and technology development required to perfect fusion propulsion devices can be carried out in the laboratory. However, ultimately, a full-scale test of fusion propulsion will be required. Fusion propulsion devices are large and heavy. The dipole configurations described in Table IV are comparable in size to a large fusion power plant, produce gigawatts of fusion power, and produce significant fluxes of energetic neutrons from the unavoidable D-D and D-T reactions. Conducting full-scale tests of such propulsion devices on earth will be challenging.

Table IV - Dipole performance for various missions

	Mars	Jupiter	Tau
One-way flight time, $\tau$ (years)	0.25	1	20
Characteristic velocity (m/s)	$1.3 \times 10^5$	$2.5 \times 10^5$	$1.1 \times 10^6$
Exhaust velocity (m/s)	$1.0 \times 10^5$	$1.8 \times 10^5$	$6.7 \times 10^5$
Mass flow rate (kg/s)	0.25	0.081	0.0055
Thrust (N)	$2.5 \times 10^4$	$1.4 \times 10^4$	$3.7 \times 10^3$
Initial mass (kg)	$5.0 \times 10^6$	$4.0 \times 10^6$	$4.8 \times 10^6$
Thrust system mass (kg)	$1.25 \times 10^6$	$1.25 \times 10^6$	$1.25 \times 10^6$
Propellant mass (kg)	$2.0 \times 10^6$	$2.6 \times 10^6$	$3.5 \times 10^6$
Payload mass (kg)	$1.8 \times 10^6$	$2.3 \times 10^5$	$5.4 \times 10^4$
Payload ratio	0.35	0.058	0.011
Thrust power (MW)	1250	1250	1250

The first major step in the space program proposed by E.S. President George W. Bush is the establishment of a permanent lunar settlement. When such a lunar settlement is established, it will provide an ideal location for proof-testing the dipole fusion rocket. The lunar environment provides two of the immediate requirements for magnetic fusion: vacuum and low temperature. If high-temperature superconductors are available, the need for refrigeration is further reduced. (Note, however, that once the dipole starts operation, due to neutron heating, the central coil will require cooling, independent of the surrounding temperature). An additional advantage of an established lunar settlement would be the availability of an infrastructure and people to conduct experiments and to modify equipment as required.

The low-gravity environment of the moon is an attractive place in which to construct and test the dipole rocket. Large component can be handled more easily on the lunar surface. Furthermore the lunar soil is a potential source of the  $^3\text{He}$  fuel. Ultimately, when the prototype rocket is ready for flight testing, the lunar surface will be an attractive base from which to launch it. Since the moon's gravity is much less than that of Earth, the thrust needed to escape the moon is correspondingly less,

and the stresses induced during launch would be reduced accordingly. Thus the structure of the rocket can be lighter and simpler if it is constructed for lunar launching.

One of the specific advantages displayed by MFE propulsion is the possibility of tuning the exhaust velocity during travel, as demonstrated by Fig. 8 for a 3-month trip to Mars.

#### 4.5 - MFE FUSION REACTOR DESIGNS FOR SPACE APPLICATIONS

Conceptual designs of magnetic fusion reactors for space propulsion during the past decade have generally calculated specific powers of 1-10 kW thrust/kg

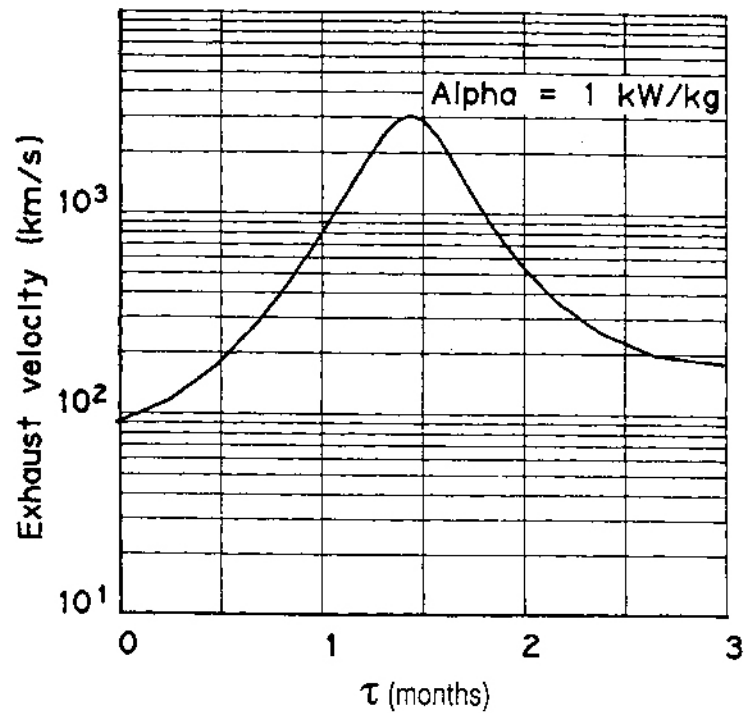


**Figure 8** - Exhaust velocity variation on a 3-month transfer trajectory to Mars (based on Stuhlinger, Ref. [5])

Table V - MFE Configurations

First Author	Year	Configuration	Specific Power (kW/kg)
--------------	------	---------------	---------------------------

Borowski	1987	Spheromak	10.5
Santarius	1988	Tandem Mirror	1.3
Chapman	1989	FRC	--
Haloulakis	1989	Colliding Spheromaks	--
Bussard	1990	Riggatron Tokamak	3.9
Bussard	1990	Inertial-Electrostatic	>10
Teller	1991	Dipole	1.0
Carpenter	1992	Tandem Mirror	4.3
Nakashima	1994	FRC	1.0
Kammash	1995	Gas Dynamic Trap	21 (D-T)
Kammash	1995	Gas Dynamic Trap	6.4 (D- <sup>3</sup> He)

Various MFE configurations have been considered for space applications. Generally, the key features contributing to an attractive design are

- λ D-<sup>3</sup>He fuel
- λ Solenoidal magnet geometry (linear reactor geometry) for the coils producing the vacuum (without plasma ) magnetic field.
- λ Advanced fusion concepts that achieve high values of the parameter beta (ratio of plasma pressure to magnetic-field pressure).

The projected specific powers for selected designs appear in the table V below, widely varying assumptions and levels of optimism have gone into the conceptual designs and the resulting specific powers.

## 5 - INERTIAL FUSION ENERGY (IFE)

The possibility of igniting thermonuclear micro-explosions with pulsed laser beams was first proposed by Basov and Krokhin in 1963. The idea of using for the same purpose intense beams of charged heavy particles accelerated in conventional linear high energy particle accelerators was proposed at about the same time [6]. Corresponding heavy ion drivers used in a so-called direct drive compression of the pellet containing DT fuel have been extensively reviewed [7].

The suggestion of a rocket motor to be driven by a chain of explosions was first proposed by Ganswindt in Germany around 1891 [8]. Following the discovery of nuclear explosives by Hahn, Meitner and Strassmann in 1938 this idea was revived around 1950 by Everett and Ulam, two Los Alamos scientists, and a feasibility study under the name Project Orion was made. In this particular concept it was intended to explode a chain of small fission bombs behind a pusher plate, which prior to each explosion would have to be covered by a layer of a liquide, for example water, to protect it from the intense heat generated by the fission explosive. In this way a large thrust at a high specific impulse would be imparted onto the pusher plate and hence the spacecraft. The limitation of such a propulsion system is determined by the maximum permissible temperature of  $\sim 10^5$  °K, which the evaporating liquid is permitted to attain without destroying the pusher plate. The great technical problem of such a system is the critical mass of a fission chain reaction, making it difficult to miniaturise a fission explosion. The explosive power of the fission bombs is always very large and the proposed device is therefore at the limit of technical feasibility. It is also obvious that there is no improvement if instead of fission explosives thermo-nuclear explosives, to be triggered themselves with fission explosives, are being used. If however, the fission trigger can be replaced by some other



means permitting the ignition of thermonuclear microexplosions, the situation is drastically changed for the better.

Sometimes ago, Winterberg [9] proposed to ignite microexplosions through pulse power techniques, producing intense pulsed beams of either relativistic electrons or space charge neutralised ions, which have the best chance to be successfully developed for a mobile system.

Such a proposal going back to 1968, received very recently a novel boost with the recently developed fast ignition concept (FIC). FIC has been initially proposed by Tabak *et al.* in 1994, at Livermore, and it has been recently reviewed [10]. FIC elaborates on the recently proposed ultraintense and chirped lasers which can produce highly directed and ultraintense beams of relativistic electrons in the MeV energy range. Moreover, it is also possible to convert the latter into fully neutralized proton beams in the 1-70 MeV energy range.

The emphasis on particle trigger is largely motivated by the fact that lasers by comparison have a much smaller efficiency, which for a rocket propulsion system requires a much larger waste heat rejection system.

However, with the concept of staged thermonuclear microexplosions, detailed below, the initial trigger energy conceivably can be made so small that highly efficient gas lasers, such as the CO<sub>2</sub> laser, cannot be ruled out.

Therefore, one can think of a basic IFE propulsion concept, as shown on Fig. 9

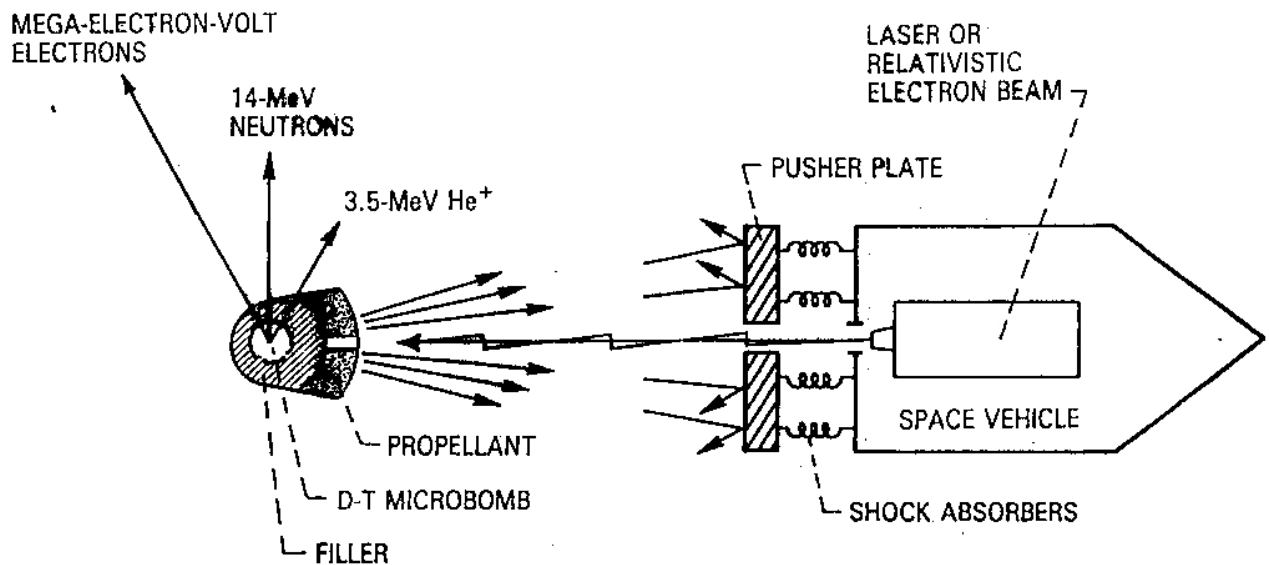


**Figure 9** - Inertial fusion propulsion system (Orion Project)

A crucial improvement for the nuclear pulse rocket concept results in combining thermonuclear microexplosion with strong magnetic reflectors. Magnetic reflectors of the required strength turn out to be feasible with superconducting magnetic field coils. The thermonuclear microexplosion reaction should preferably produce little or no neutron radiation which would penetrate into the spacecraft thereby creating in it a large heat source and which would drastically increase the heat rejection system. One good candidate meeting the requirement of low neutron radiation is again the DHe<sup>3</sup> thermonuclear reaction.

If one desires to use a thermonuclear fuel (1) which is abundant and (2) which leads only to charged fusion products, one is led to the reaction  $H + B^{11} \rightarrow {}^3He^4$ ,  $B^{11}$  is sufficiently abundant in the required amounts. The  $HB^{11}$  reaction also ideally satisfies the condition that the reaction shall only lead to charged fusion products. The next reaction in line is  $H + Li^7 \rightarrow 2He^4$ , depending on the much less abundant  $Li^7$  isotope. Under the light elements only the reaction  $H + N^{15} \rightarrow He^4 + C^{12}$  seems still promising, but it depends on the relatively rare  $N^{15}$  isotope [11].

The ignition of these reactions is much more difficult to achieve than the DT or even the  $DHe^3$  reaction. Typically ignition energies  $\sim 10^3$  larger may be required. These larger ignition necessitate a correspondingly larger energy storage system which present a serious problem for mobile propulsion systems. If however, the concept of staged thermonuclear microexplosions is used [11, 12], whereby a smaller microexplosion ignites a subsequent larger one, the ignition of such reactions as the  $HB^{11}$  reaction suddenly comes within reach. The staging of thermonuclear microexplosions may pose an economic problem for an earthbound power plant, where the cost of the thermonuclear target has to be kept low, but in case of a propulsion system no such economic considerations enter. In this concept one may use for the first stage the easily ignitable DT reaction to be followed by a second stage  $HB^{11}$  microexplosion, ignited by the first stage DT microexplosion. If the energy output of the second stage is for example  $\sim 10^2$  times larger, than for the first stage, only a small relative fraction of neutrons are produced.

One may think that the same end could also be reached by mixing DT with  $BH^{11}$ . However, because of the much higher burn rate in DT the energy released by the DT reaction will be uselessly dissipated long before the  $HB^{11}$  gets started. Furthermore, mixing a small amount of DT with a large amount of  $HB^{11}$ , as would be required to ignite a large amount of  $HB^{11}$  with a small amount of DT, would dilute the DT to such a degree that the thermonuclear ignition of the DT contained in this mixture would become very difficult. The only way out of this dilemma therefore seems to be concept of staged thermonuclear microexplosions.

There are three likely possibilities by which this may be achieved. The first possibility is based on a shock wave lens, the second on a shock wave mirror and the third one, on the adiabatic Prandtl-Meyer flow. All these three staging methods require additional material reducing the overall specific impulse. This may not pose a serious drawback in a propulsion system to serve for transportation within our planetary system, but it will in one designed for interstellar missions requiring the highest possible specific impulse in order to bring down the transit times to a few decades, less than a human lifetime. In aiming at the highest possible specific impulse we thus propose as a fourth staging principle a method based on staged magnetic reflectors produced by superconducting magnetic field coils. Technically, this is probably the most difficult way to realise staging, but the most rewarding one in terms of efficiency.

## 5.1 - STAGED THERMONUCLEAR MICROEXPLOSIONS

Let  $E_0$  be the input energy to trigger the first microexplosion and which is drawn from a pulsed laser-, electron-, or ion-beam, and let  $E_1$  be the energy released by this first microexplosion, then according to computer studies for the DT thermonuclear reaction by Nuckolls *et al.* [13] the energy gain  $E_1/E_0$  approximately follows the law

$$\frac{E_1}{E_0} \cong cE_0^{1/3} \quad [6.]$$

where  $c = \text{const.}$  This expression holds under the assumption that the thermonuclear target is compressed with part of the input energy  $E_0$  going into work for compression. For uncompressed solid DT targets the breakeven energy is  $\sim 10^6$  Joule.

In a staged microexplosion, only the energy released in the form of charged fusion products can be coupled to the next larger microexplosion target. In the DT reaction only 20% of the released energy

goes into charged fusion products. Furthermore, a substantial amount of energy will go into the material of the shock wave lens or mirror, refocusing the energy released in the form of charged fusion products onto the following target. If the fraction of the energy released into charged fusion products is  $e_1$  and if the fraction of this energy reaching the following target is  $e_2$ , the energy  $E_1^*$  available for the ignition of the following microexplosion is then given by

$$\frac{E_1^*}{E_o} = e_1 e_2 c E_o^{1/3} \quad [7.]$$

For the DT reaction  $e_1 = 0.2$ , but for the HB<sup>11</sup> reaction  $e_1 = 1$ . The value of  $e_2$  is more difficult to assess. For magnetic reflectors  $e_2 = 1$  ideally, but in the cases of material lenses or reflectors  $e_2 < 1$ . For material reflectors one may roughly assume that  $e_2 \approx 0.5$ . In the case of lenses the losses can be expected to be bigger and hence  $e_2$  smaller.

In generalising Eq. (7), the energy  $E_n^*$  released by the  $n$ th microexplosion (expressed in terms of  $E_{n-1}^*$ ), and which can be coupled to the  $(n + 1)$  th microexplosion target, is given by

$$\frac{E_n^*}{E_{n-1}^*} = e_1 e_2 c E_{n-1}^{*1/3} \quad [8.]$$

or

$$E_n^* = e_1 e_2 c E_{n-1}^\alpha \quad \text{where } \alpha = 4/3 \quad [9.]$$

$$\frac{E_n^*}{E_o} = (e_1 e_2 c)^{\beta(n)} E_o^{\alpha^n - 1} \quad \text{where } \beta(n) = \sum_{m=0}^{n-1} \alpha^m \quad [10.]$$

From there, the total energy output  $E_n$  of the  $n$ th microexplosion, which includes the energy going into neutrons and dissipated in the material of the shockwave lens or mirror, is obtained by multiplying this result with the factor  $(e_1 e_2)^{-1}$ , hence

$$\frac{E_n}{E_o} = (e_1 e_2)^{-1} (e_1 e_2 c)^{\beta(n)} E_o^{\alpha^n - 1} \quad [11.]$$

The total energy output  $E_{\text{tot}}$  of an  $n$ -staged microexplosion is then finally obtained by summation of the energy released in all  $n$  stages, hence

$$E_{\text{tot}} = (e_1 e_2)^{-1} \sum_{n=0}^n (e_1 e_2 c)^{\beta(n)} E_o^{\alpha^n} \quad [12.]$$

## 5.2 - METHODS FOR STAGING THERMONUCLEAR MICROEXPLOSIONS

The first microexplosion would have to be ignited by one of the many proposed methods described in the literature, for example by the ablation driven implosion process, described by Nuckolls *et al.* [13], or by the ablation free implosion method, using energy focusing by reflection from a curved wall [12].

The energy released in one microexplosion has the form of a divergent blast wave. To use the kinetic energy of this divergent blast wave to ignite a subsequent microexplosion it has been redirected into a convergent wave to be aimed at a subsequent microexplosion target. One way or how this can be done is shown in Fig. 10 representing a blast wave lens. The input energy  $E_o$  coming from a laser, -electron- or ion-beam ignites microexplosion target I. After ignition the blast wave from I is confined by the material wall W having the form of a heart shaped body. Inside this body and parallel to its surface, but separated from it by a gap A is some material B, which for example may be a plastic foam and in which the blast wave from I will propagate with a somewhat smaller velocity than in the gap

space A. One part of the blast wave then propagates inside the gap space A and parallel to the inner surface of the heart shaped wall. The other part of the blast wave propagates with a somewhat smaller velocity in the material B. We want the energy of the blast wave from microexplosion I to converge three-dimensionally and with spherical symmetry onto the second stage microexplosion target II. This condition determines the wall shape. It requires that the sum T of the times for the individual blast wave propagating along the gap space A originating from the position a ( $r_0, \phi = \pi$ ) to the arbitrary position b ( $r, \phi$ ) and from there through the medium B to the position  $r = 0$ , are the same for all blast waves.  $r_0$  is the separation distance in between the microexplosion targets I and II of the first and second stage. This leads to the equation for the wall shape

$$r = r_0 \exp[(\phi - \pi) / \sqrt{e_2 - 1}] \quad [13.]$$

which is a logarithmic spiral rotated around the axis connecting target I with target II.

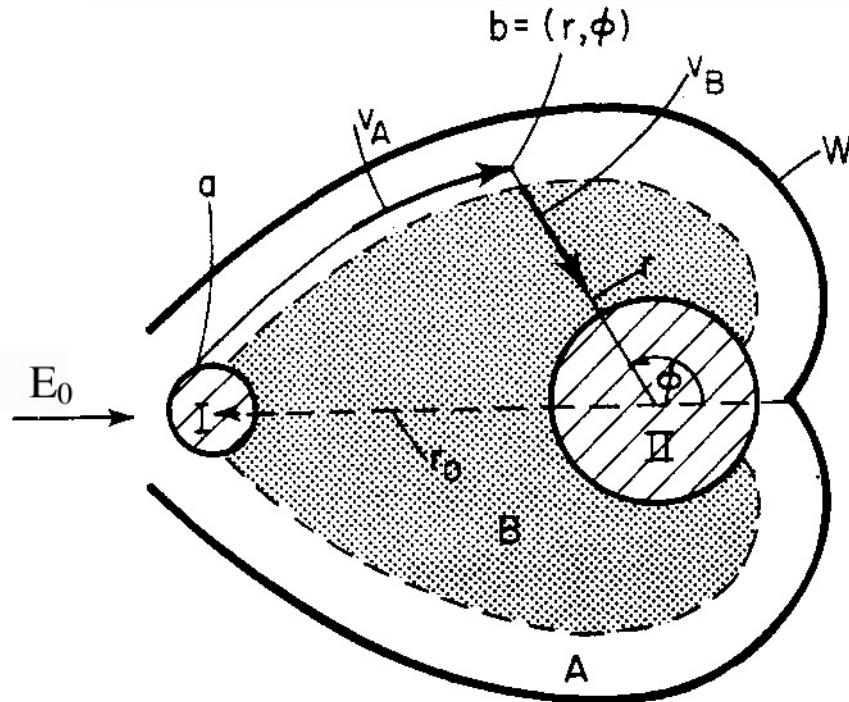


**Figure 10** - Explosive lens for two stage thermonuclear microexplosion. I first, II second stage target; W heart shaped wall; A gap space with blast velocity  $v_A$ , B medium with blast velocity  $v_B$ ;  $r, \phi$  polar coordinates;  $E_0$  input energy to ignite I;  $r_0$  distance from I to II.

In Fig. 11 the example of a three stage microexplosion target shows how this same principle can be used to build a multistage target, by encapsulation of the first wall  $W_1$  into a second wall  $W_2$ , whereby under the blast wave of microexplosion II the wall  $W_1$  collapses, focusing the energy of microexplosion II onto target III.

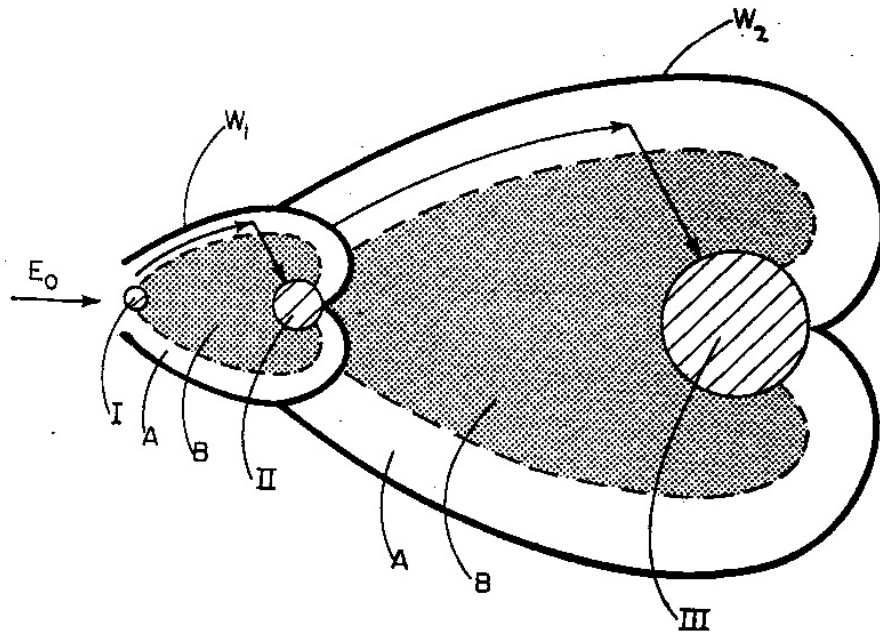


**Figure 11** - Three stage thermonuclear microexplosion target employing the explosive lens technique. I, II, III first, second and third stage; Gap A and medium B with blast velocity  $v_A$  and  $v_B$ ;  $W_1$ ,  $W_2$  walls;  $E_0$  input energy to ignite I

The concept of the explosive lens technique for staging microexplosions has the disadvantage that much of the energy is uselessly dissipated into the lens material B and therefore lost for igniting the following target, leading in Eq. (8) to a small values of  $e_2$ . As in optics, where one can use mirrors in place of a lens with less absorption losses, one can likewise do the same here. A two stage microexplosion target doing this is shown in Fig. 12.

The trigger energy ignites target I which upon detonation sends out a spherically divergent blast wave to be reflected from the curved egg-shaped wall and thereby be refocused onto target II. Again, from the condition that the reflected blast wave is of spherical symmetry with respect to the target II one can determine the wall shape. It is clear that in case of sound waves, to be reflected under the same angle as the incident wave, the shape would be simply an ellipsoid. In the case of a shock wave, however, not obeying such a simple reflection law, the wall shape can substantially deviate from the one of an ellipsoid.

Finally, Winterberg [11] also proposed a method of staging involving only magnetic reflectors. In this method then ideally  $e_2 = 1$ .

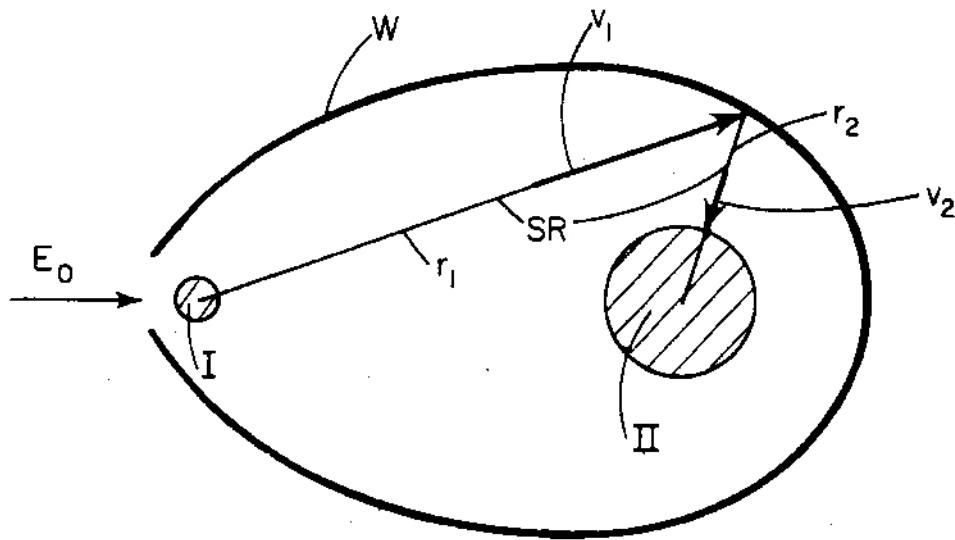


**Figure 12** - Shock wave mirror for two stage thermonuclear microexplosion. I first, II second stage target; W egg shaped wall; SR blast wave ray from I to II,  $v_1$  velocity of incident and  $v_2$  of reflected wave;  $r_1$ ,  $r_2$  bipolar coordinates centred in I and II;  $E_0$  input energy to ignite I.

The idea is explained for the example of a three stage microexplosion in Fig. 13.

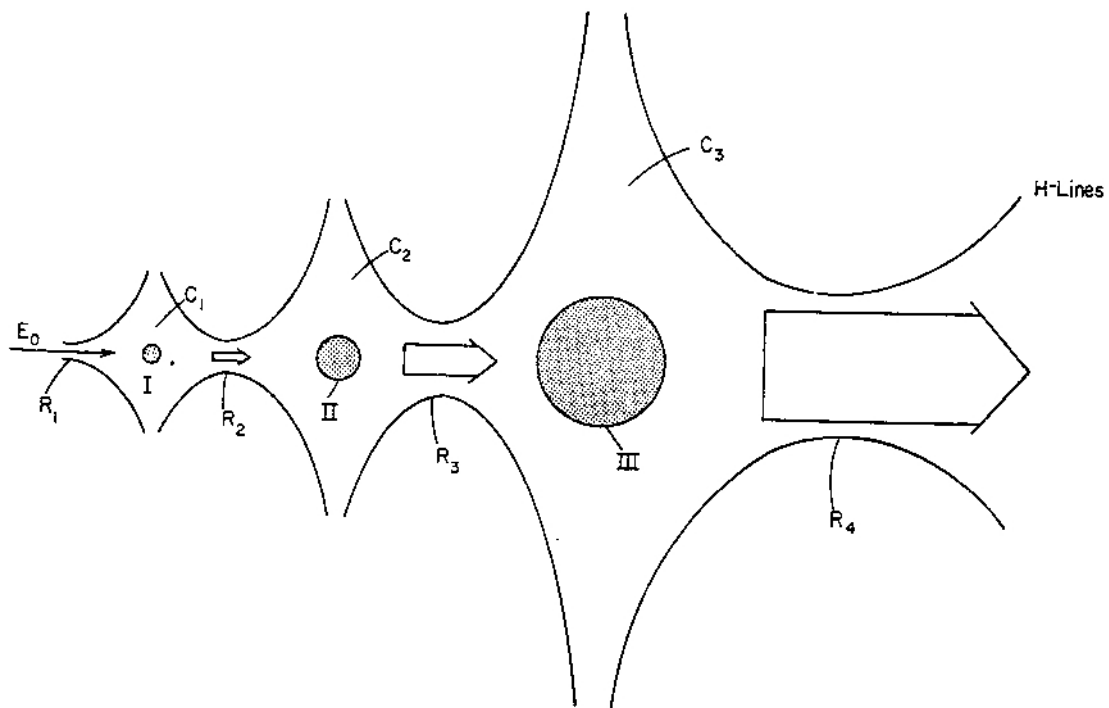


**Figure 13** - Three stage thermonuclear microexplosion target using magnetic reflectors. I, II, III first, second and third stage;  $C_1$ ,  $C_2$ ,  $C_3$  magnetic cusps;  $R_1$ ,  $R_2$ ,  $R_3$  magnetic mirrors;  $E_0$  input energy to ignite I.

After igniting the first stage I, the blast wave from microexplosion I, confined in the magnetic cusp  $C_1$ , will be reflected from the small magnetic mirror  $R_1$  but will pass through the larger magnetic mirror  $R_2$  entering the cusp  $C_2$  where it is reflected from its wall and thereby focused onto target II. After the ignition of target II the blast wave from this microexplosion will then enter cusp  $C_3$  bombarding target III. The debris from this three staged microexplosion will finally pass through the magnetic mirror  $R_4$  to be transformed into thrust.

In order for such a system to be feasible, the magnetic pressure must be strong enough to withstand the stagnation pressure of the microexplosion. Since the final stage microexplosion is the largest one it will give an upper limit for the size of the magnetic cusp confining the last stage. The cusp sizes for the lower stages are then always smaller. If the energy of the last stage microexplosion is  $E_n$  and the average cusp radius  $R_n$ , the minimum magnetic field strength is determined by the inequality ( $E_n$  in ergs).

$$\frac{H^2}{8\pi} \frac{4\pi}{3} R_n^3 > E_n$$

or for a given value of  $H$  the minimum cusp radius is determined by

$$R_n > \sqrt[3]{6E_n/H^2}$$

Let us assume that  $E_n \sim 10^{10} \text{ J} = 10^{17} \text{ ergs}$ , which is in line with the estimates made above. Let us assume that  $H \sim 3 \times 10^5 \text{ G}$  accessible to superconducting magnets. It then follows that  $R \geq 2\text{m}$ , a very reasonable value. The present cascade approach has recently been revisited with fast ignition concepts [14].

## 6 - MATTER-ANTIMATTER ANNIHILATION

### 6.1 - GENERAL

Devotees of Star Trek will need no reminding that the starships *Enterprise* and *Voyager* are powered by engines that utilize antimatter. Far from being fictional, the idea of propelling spacecraft by the annihilation of matter and antimatter is being actively investigated at NASA's Marshall Space Flight Center, Pennsylvania State University, and elsewhere. The principle is simple: an equal mixture of matter and antimatter provides the highest energy density of any known propellant. Whereas the most efficient chemical reactions produce about  $1 \times 10^7 \text{ joules (J)/kg}$ , nuclear fission  $8 \times 10^{13} \text{ J/kg}$ , and nuclear fusion  $3 \times 10^{14} \text{ J/kg}$ , the complete annihilation of matter and antimatter, according to Einstein's mass-energy relationship ( $E = mc^2$ ), yields  $9 \times 10^{16} \text{ J/kg}$ . In other words, kilogram for kilogram, matter-antimatter annihilation releases about ten billion times more energy than the hydrogen/oxygen mixture that powers the Space Shuttle main engines and 300 times more than the fusion reactions at the Sun's core. However, there are several technical hurdles to be overcome before an antimatter rocket can be built. The first is that antimatter does not exist in significant amounts in nature—at least, not anywhere near the solar system. It has to be manufactured. Currently only way to do this is by energetic collisions in giant particle accelerators, such as those at FermiLab, near Chicago, and a CERN, in Switzerland. The process typically involves accelerating protons to almost the speed of light and then slamming them into a target made of a metal such as tungsten. The fast-moving protons are slowed or stopped by collisions with the nuclei of the target atoms, and the protons kinetic energy converted into matter in the form of various subatomic particles, some of which are antiprotons—the simplest form of various subatomic particles. So efficient is matter-antimatter annihilation that 71 milligrams of antimatter would produce as much energy as that stored

by all the fuel in the Space Shuttle external tank, Unfortunately, the annual amount of antimatter (in the form of antiprotons) presently produced at Fermilab and CERN is only 1-10 nanograms [15].

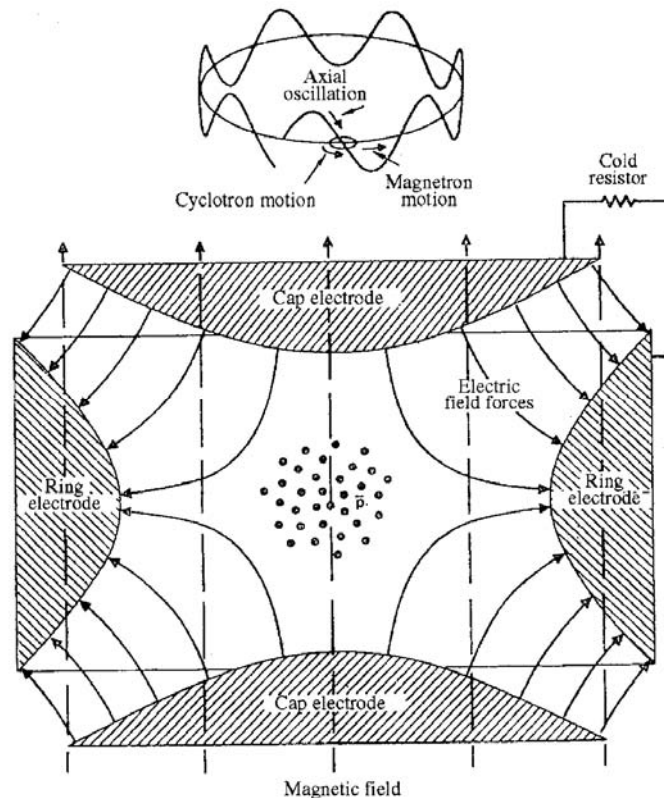


**Figure 14** - Penning trap antiprotons ions

On top of this production shortfall, there is the problem of storage. Antimatter cannot be kept in a normal container because it will annihilate instantly on coming into contact with the container's walls. One solution is the Penning Trap—a supercold, evacuated electromagnetic bottle in which charged particles of antimatter can be suspended. Antielectrons, or positrons, are difficult to store in this way, so antiprotons are stored instead. Penn State and NASA scientists have already built such a device capable of holding 10 million antiprotons for a week. Now they are developing a Penning Trap with a capacity 100 times greater [16]. Basic features of a Penning Trap are depicted on Fig. 14.

At the same time, Fermilab is installing new equipment that will boost its production of antimatter by a factor of 10-100.

A spacecraft propulsion system that works by expelling the products of direct one-to-one annihilation of protons and antiprotons—a so-called beamed core engine (Fig. 15) would need 1-1,000 grams of antimatter for an interplanetary or Interstellar journey [1,17].

Even with the improved antiproton production and storage capacities expected soon, this amount of antimatter is beyond our reach. However, the antimatter group at Penn State has proposed a highly efficient space propulsion system that would need only a tiny fraction of the antimatter consumed by a beamed core engine. It would work by a process called antiproton-catalyzed microfission/fusion (ACMF) [18,20].



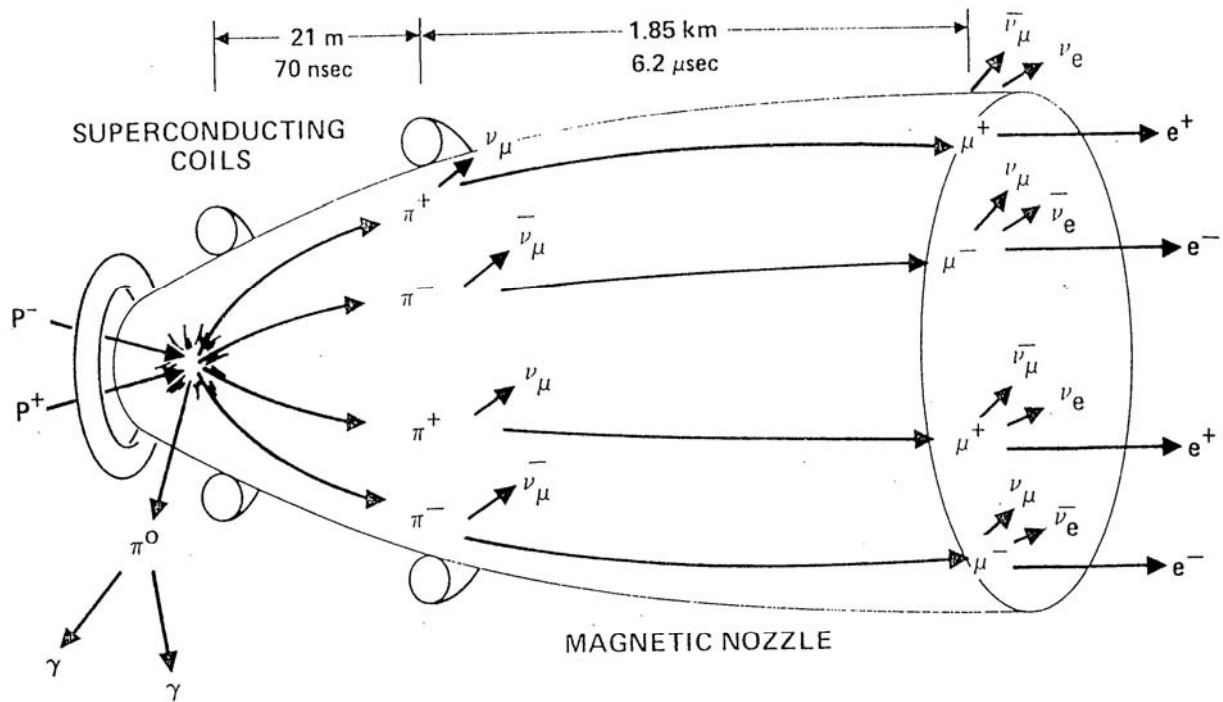


**Figure 15** - Schematic of an idealized antiproton rocket. (Beamed Core Engine)

## 6.2 - ACMF AND ICAN-II

Antimatter annihilation, nuclear fission, and nuclear fusion all have major problems. Antimatter annihilation requires antimatter, which is hard to come by in this matter filled world. Fission produces a lot radioactive waste, as well as being the least efficient of the three. Fusion is hard to get started, and sustain (the Sun is able to sustain its fusion reaction only because of its immense gravitational field). However, in a wonderful example of the sum of the parts not being equal to the whole, by combining these three problematic energy source, all of these problems are minimized. Very little antimatter is needed (just enough to start the fission reaction), very little fission occurs (just enough to start the fusion reaction), and the fusion reaction doesn't have to be sustained for very long (the drive uses *pulses* of thrust). It has already been well demonstrated that a fission reaction can be sufficient to ignite a fusion reaction (i.e. the Hydrogen Bomb), and Penn State has recently demonstrated that a relatively small number of antiprotons can be used to ignite a fission reaction.

A pellet of Deuterium, Tritium, and Uranium-238 (nine parts D-T for every one part U-238) is injected into the reaction chamber. First the pellet is compressed using ion particle beams, then irradiated with a 2ns burst of antiprotons. The antiprotons annihilate some of the pellet, producing enough energy to cause the U-238 to fission. In turn, the fission reaction ignites a fusion reaction within the Deuterium-Tritium (D-T) core. The fusion reaction produces the desired engine thrust. A new pellet is than inserted, and the process repeats itself (see Fig. 16).

The antiproton triggering of the process is made easier by annihilation within  $U^{235}$  pastille initially stopping antiproton beam.

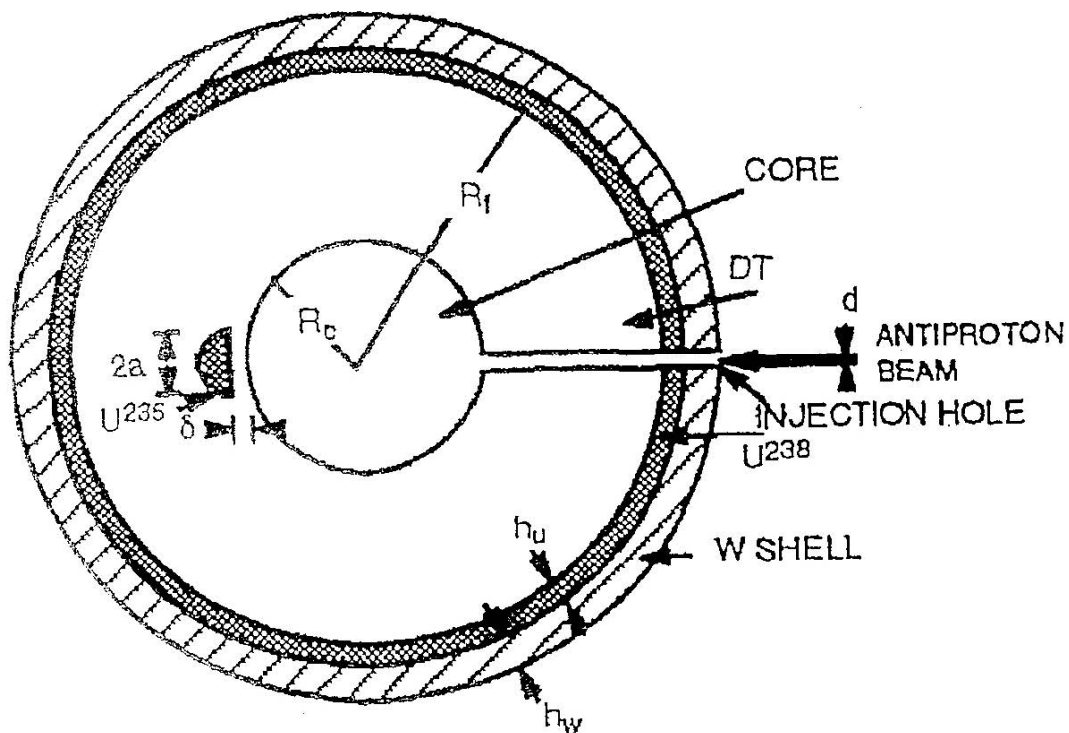


Figure 16 - Pellet construction and geometry

The drive concept seems to be the most efficient (as determined by NASA) for use in manned, planetary missions. A round-trip, manned mission to Mars using the ACMF drive would only take 120 days, and require approximately 140 nanograms of antimatter (which could be produced in one year by Fermilab after a few major upgrades are implemented). In addition, it would require approximately 362 metric tons of propellant (the D-T-U pellets).

Penn State University has designed a spacecraft, called ICAN-II, that would use the ACMF drive for omnplanetary mission within the Solar system. Below, is a rendering of what the ICAN-II spacecraft would look (see Fig. 17) like if built.

ICAN-II is similar to the ORION spacecraft design put forth by Stanislaw Ulam in the late 1950 [19]. The ORION was intended to be used to send humans to Mars and Venus by 1968. It was to utilize a large number of nuclear bombs that would be set off one after the other, behind the ship to push it forward. It would, of course, require large shock-absorbers and ablative shielding for its pusher-plate. The ICAN-II also, in a sense, utilizes nuclear "bombs" for thrust. However, instead of regular fission bombs like the ORION would utilize ICAN-II uses what are, essentially, a large number of very small hydrogen-bombs. Set off, of course, by a stream of antiprotons. Ecological concerns would probably require that ICAN-II be assembled in space. Of course, a precedent for such large scale orbit-based assembly is already being set by the construction of the International Space Station.

The radiation from ICAN-II's ACMF engine would be intercepted by a 4 meter radius silicon carbide shell. Additionally, 1.2 meters of lithium hydride will shield the fuel rings from high-energy neutrons that are ejected from the nuclear explosions, and 2.2 meters of shielding will protect the crew modules. The spacecraft would have a total mass of 625 metric tons, with 82 additional metric tons available for payload. This is more than sufficient to carry a Mars Lander and exploration vehicles.

The ICAN-II is a viable spacecraft design that could be built within the next two decades. Currently, antiprotons can only be stored for a few weeks and production is very low; but, the problems with the storage and production are engineering problems, not physical problems.

Estimates of component masses for a return trip 120 day,  $\Delta V = 100$  km/s Mars mission (RT) are shown in Table VI

Table VI - Estimate of ICAN-II Vehicle Masses for 120 days,  
 $\Delta V = 100$  km/s Mars/Mission (RT)

Component	Mass (metric tons)
Ion Driver	100
Engine Structure	27
Spacecraft Structure	30
Antiproton Traps	5
Neutron Shielding	45
Power Processing	58
Payload on ICAN	20
Mars Lander/Surface Payload	53
<u>Mars Mission Ascent Vehicle</u>	<u>9</u>
Total Dry Mass	345
<u>Mass of Silicon Carbide Thrust Shell</u>	<u>362</u>
Total Mass of ICAN	707

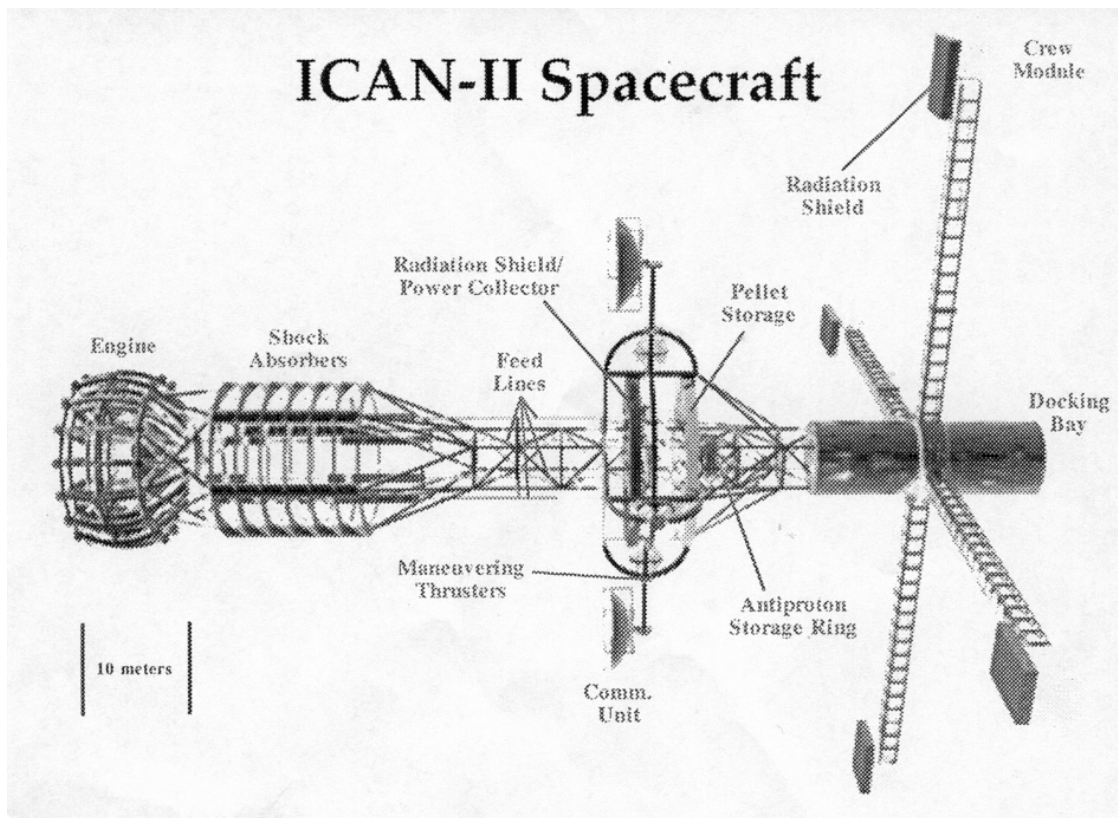


Figure 17 - ICAN-II project

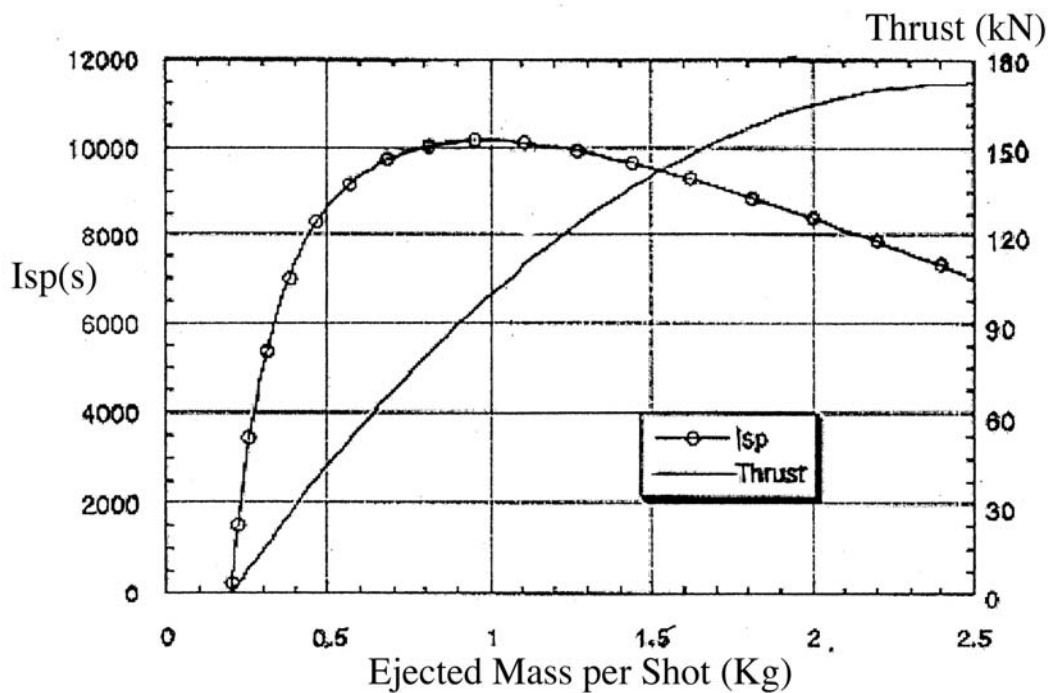




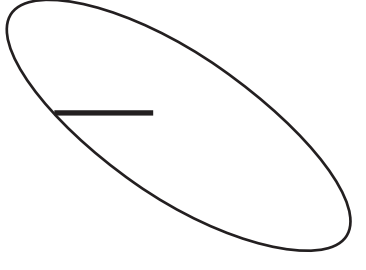
Figure 18 - Thrust and Isp Versus Propellant at 1 Hz.

Figure 18 shows the thrust and ISP for a 1 Hz firing rate. For a  $\Delta V$  of 100 km/sec and an Isp of 13,500 seconds (200 g WLS), 362 metric tons of propellant are required for a 345 metric tons ICAN II dry mass (see table VI). With a 200 g WLS, the thrust is about 100 kN, which accelerates the

outbound craft to a 25 km/sec  $\Delta V$  in 3 days. For 800 g of ejected mass, about 30 ng of antiprotons are required. Hence, ICAN-II could be fueled with one year's production of antiprotons at Fermilab, estimates to be approximately 140 ng by the year 2010.

Utilizing vehicle performance parameters presented above, three potential ICAN-II missions were analyzed [20]. As an intermediate step to a full non-impulsive analysis, simulations of vehicle trajectories within planetary gravitational spheres of influence were performed by modeling vehicle thrust and solar gravity as perturbations. The results indicate that the majority of the  $\Delta V$  was gained within the planetary spheres of influence, permitting the design of interplanetary trajectories using impulsive maneuvers at the endpoints. Missions to Mars, Jupiter and Pluto were investigated, and the results are presented in Table VII. The short transfer times significantly alleviate psychological and physical dangers to the crew. A total  $\Delta V$  requirement of 120 km/s was stipulated to provide a large launch window every two years, although the mission can be completed with as little as 70 km/s if departure is timed correctly.

Table VII - Examples of ICAN-II capabilities

Mission	$\Delta V$ (km/s)	Window	Trajectory
Earth-Mars - Round Trip - 30 day Stay - 120 day Total	120 km/s	~ 3 mos. every 2 years	
Earth-Jupiter -Round Trip - 90 day Stay - 18 months Total	100 km/s	~ 1.5 mos. every year	
Earth-Pluto - One way - 3 years	80 km/s	~ 2.5 mos. every year	

Whereas conventional nuclear fission can only transfer heat energy from a uranium core to surrounding chemical propellant, ACMF permits all energy from fission reactions to be used for

propulsion. The result is a more efficient engine that could be used for interplanetary manned missions. The ICAN-II (ion compressed antimatter nuclear II) spacecraft designed at Penn State would use the ACMF engine and only 140 nanograms of antimatter for a manned 30-day crossing to Mars.

A follow-up to ACMF and ICAN is a spacecraft propelled by AIM (antiproton initiated microfission/fusion) in which a small concentration of antimatter and fissionable material would be used to spark a microfusion reaction with nearby material. Using 30-130 micrograms of antimatter, an unmanned AIM-powered probe -AIMStar- would be able to travel to the Oort Cloud in 50 years, while a greater supply of antiprotons might bring Alpha Centauri within reach.

Combining antimatter technology with the concept of the space sail has also led to the idea of the antimatter-driven sail [22].

### 6.3 - ANTIMATTER PROPULSION CONCEPTS

In view of the important energy losses arising in the  $p - \bar{p}$  annihilation through ultimate neutrino energy production ( $\sim 50\%$  of total reaction energy, see Fig. 15) an important aspect of all antimatter-powered propulsion concepts is to utilize the products as soon as possible after the original  $\bar{p}p$  reaction, when most of the product energy is tied up in a charge state. This entails either (1) using the products to heat a reaction fluid through fluid/product collisions or an intermediate material, or (2) directing the highly energetic charged pions or muons out a magnetic nozzle to produce thrust. The propulsion concepts that employ these mechanisms generally fall into four categories: (1) solid core, (2) gaseous core, (3) plasma core, and (4) beamed core configurations.

The solid core concept [22],[23] uses antiprotons to heat a solid, high-atomic weight ( $Z$ ), refractory metal core. Propellant is pumped into the hot core and expanded through a nozzle to generate thrust. The performance of this concept is roughly equivalent to that of the nuclear thermal rocket ( $I_{sp} \sim 10^3$  sec) due to temperature limitations of the solid. However, the antimatter energy conversion and heating efficiencies are typically high due to the short mean path between collisions with core atoms ( $\eta_e \sim 85\%$ ).

The gaseous core system [22-24] substitutes the low-melting point solid with a high temperature gas, thus permitting higher operational temperatures and performance ( $I_{sp} \sim 2 \times 10^3$  sec). However, the longer mean free path for thermalization and absorption results in much lower energy conversion efficiencies ( $\eta_e \sim 35\%$ ).

One step beyond this concept is the plasma core [22-24], where the gas is allowed to ionize and operate at even higher effective temperatures. Heat loss is suppressed by magnetic confinement in the reaction chamber and nozzle. Although performance is extremely high ( $I_{sp} \sim 10^4$ - $10^5$  sec), the long mean free path results in very low energy utilization ( $\eta_e \sim 10\%$ ).

The "ultimate" system is the beamed core concept [1,17,24,25] which avoids the problems of heating a secondary fluid altogether (see Fig. 15). Here the charged products of the proton-antiproton annihilation are directly expelled out of the vehicle along an axial magnetic field. The exhaust velocities of these products are exceptionally high ( $I_{sp} \sim 10^7$  sec), approaching the speed of light. Although energy utilization efficiencies are also high ( $\eta_e \sim 60\%$ ), the flow rate and thrusts are typically very low.

In addition to these pure-antimatter systems, there are several concepts which utilize antiprotons as a driver to catalyze and initiate a hybrid fission/fusion process (Sec. 6.2) in a compressed plasma or condensed material target. Practically all of the propulsive energy in these cases is derived from fusion reactions. Consequently, antimatter requirements are much lower than those of pure-antimatter systems.

The first of such processes is Antimatter-Catalyzed Micro-Fusion/Fusion (ACMF), detailed at length in Sec. 6.2. Here a pellet of D-T and U-238 is compressed with particle beam and irradiated

with a low-intensity beam of antiprotons. The antiprotons are readily absorbed by the U-238 and initiate a hyper-neutronic fission process that rapidly heats and ignites the D-T core. The heated fission and fusion products expand to produce thrust, but the inherent isotropy of the flow results in a lower effective energy utilization and jet efficiency. Although additional thrust is obtained from an ablating surface that absorbs neutrons and electromagnetic radiation from the ignited pellet, the performance of this concept is lower than the plasma and beamed core rockets ( $I_{sp} \sim 13,500$  sec). Gaidos *et al.* [20] have shown that the interaction between the antiproton beam and target exhibits extremely high-gain yielding a ratio of fusion energy to antimatter rest mass energy,  $\beta$ , of  $1.6 \times 10^7$ . However, energy utilization is also lower due to the isotropic expansion process ( $\eta_e \sim 15\%$ ). Assuming a 3-order of magnitude improvement in the efficiency of producing antiprotons over current values, the net energy gain is 640.

#### 6.4 - AIM STAR

Another concept is Antimatter-Initiated Microfusion (AIM) [26]. Here a non neutral plasma of antiprotons within a special Penning trap is repetitively compressed via combined electric and magnetic fields. Droplets containing D-T or D-He<sup>3</sup> mixed with a small concentration of a metal, such as Pb-208 or U-238, are synchronously injected into the plasma (see Fig. 19). The main mechanism for heating the liquid droplet is antimatter-induced fission fragments which have a range of 45 microns ( $\mu\text{m}$ ) in the droplet. The power density released by the fission fragments into the D-T or D-He<sup>3</sup> is about  $5 \times 10^{13}$  W/cm<sup>3</sup>, which is enough to completely ionize and heat the fuel atoms to fusion ignition. The heated products are directed out magnetic field lines to produce thrust. The  $I_{sp}$  and energy efficiency for this concept are higher than ACMF ( $I_{sp} \sim 67,000$  sec and  $\eta_e \sim 84\%$  with D-He<sup>3</sup>, and  $I_{sp} \sim 61,000$  sec and  $\eta_e \sim 69\%$  with D-T). The gains  $\beta$  are 10 for D-He<sup>3</sup> and  $2.2 \times 10^4$  for D-T. Again assuming a 3-order of magnitude improvement in antiproton production efficiency, these gains are near breakeven in terms of net energy flow.

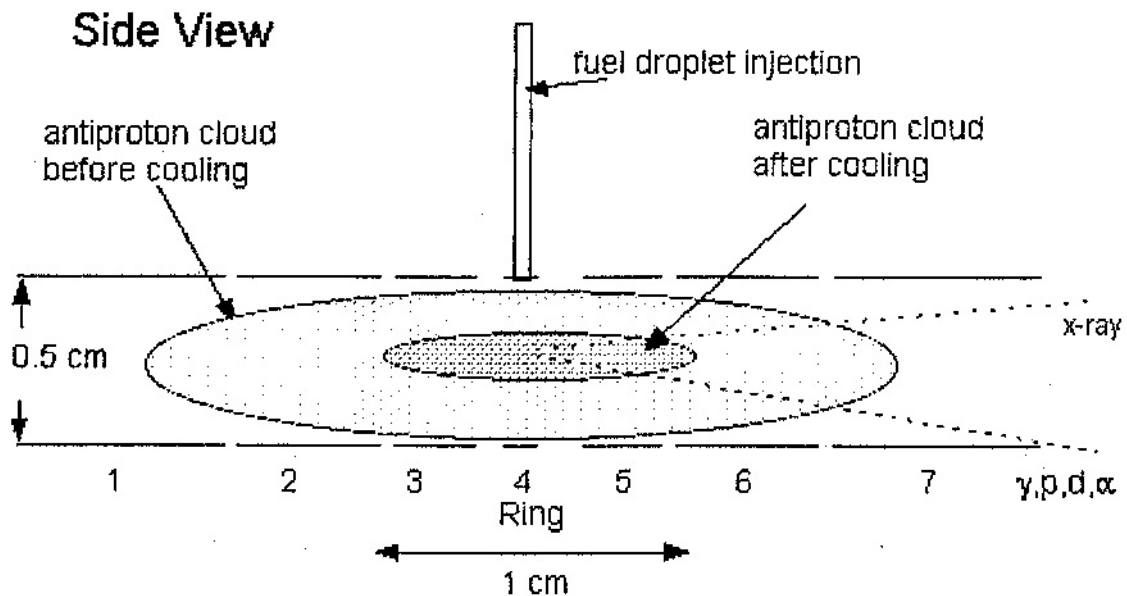


**Figure 19** - Expanded side view of the AIMStar reaction trap [R.A. Lewis *et al.* [26]]

Typical parameters for missions to Oort cloud are given in Table VIII.

Table VIII - AIMStar 50 year Mission to 10,000 A.U.

	DT	DHe <sup>3</sup>
$\Delta V$	956 km/s	956 km/s
$V_e$	$5.98 \text{ H } 10^5 \text{ m/s}$	$5.98 \text{ H } 10^5 \text{ m/s}$
$I_{sp}$	61,000 s	61,000 s
Power	33 MW	0.75 M
$T_{jrust}$	55.2 N	1.25 N
$dm/dt$	$9.22 \text{ H } 10^{-5} \text{ kg/s}$	$2.09 \text{ H } 10^{-6} \text{ kg/s}$
$t_b$	0.50 yr = 6 mo.	22 yr
Distance@burnout	37 AU	1635 AU
$\alpha_{ave}$	30.5 kW/Kg	0.69 kW/kg
$N_{pbar}$	130 $\mu\text{g}$	28.5 $\mu\text{g}$

A possible AIMStar design is depicted on Fig. 20 as an automatic vehicle

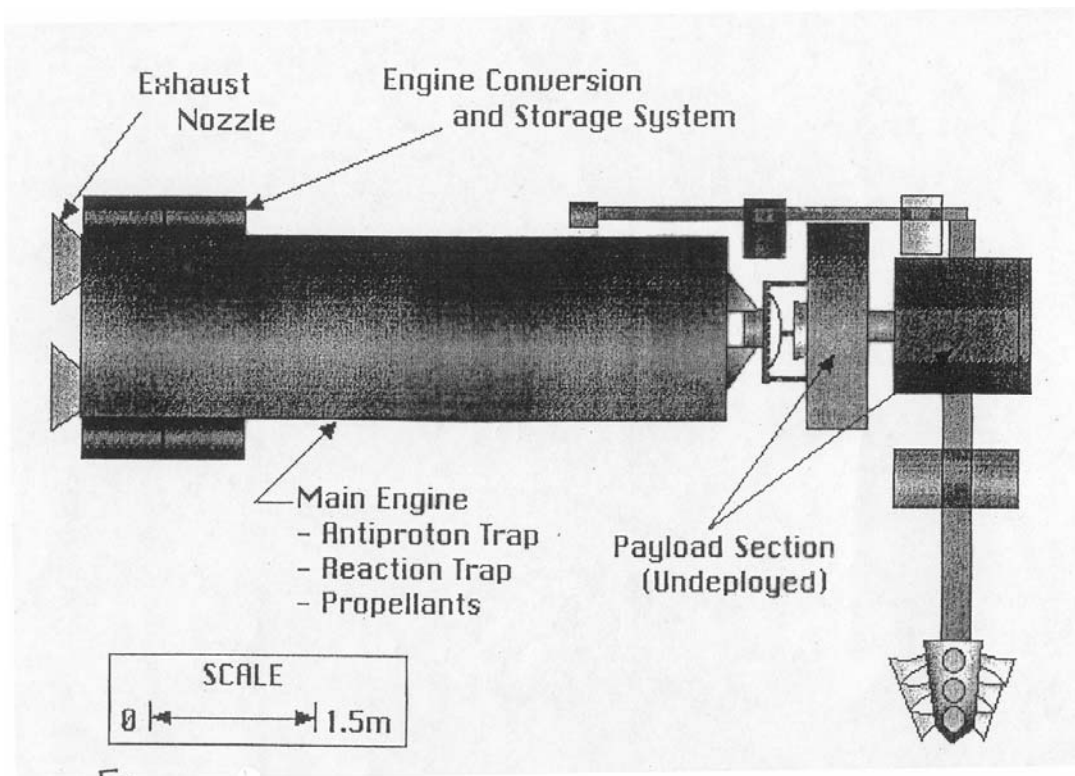




**Figure 20** - Profile of the AIMStar spacecraft

Figure 21 shows the ratio of antimatter mass to vehicle dry mass for each concept over the  $\Delta V$  range. For missions within the solar system and into near interstellar space, antimatter requirements for the catalyzed concepts are many orders of magnitude lower than their pure antimatter counterparts. At a point well beyond the solar system and when considering missions to interstellar space, beamed core becomes superior.

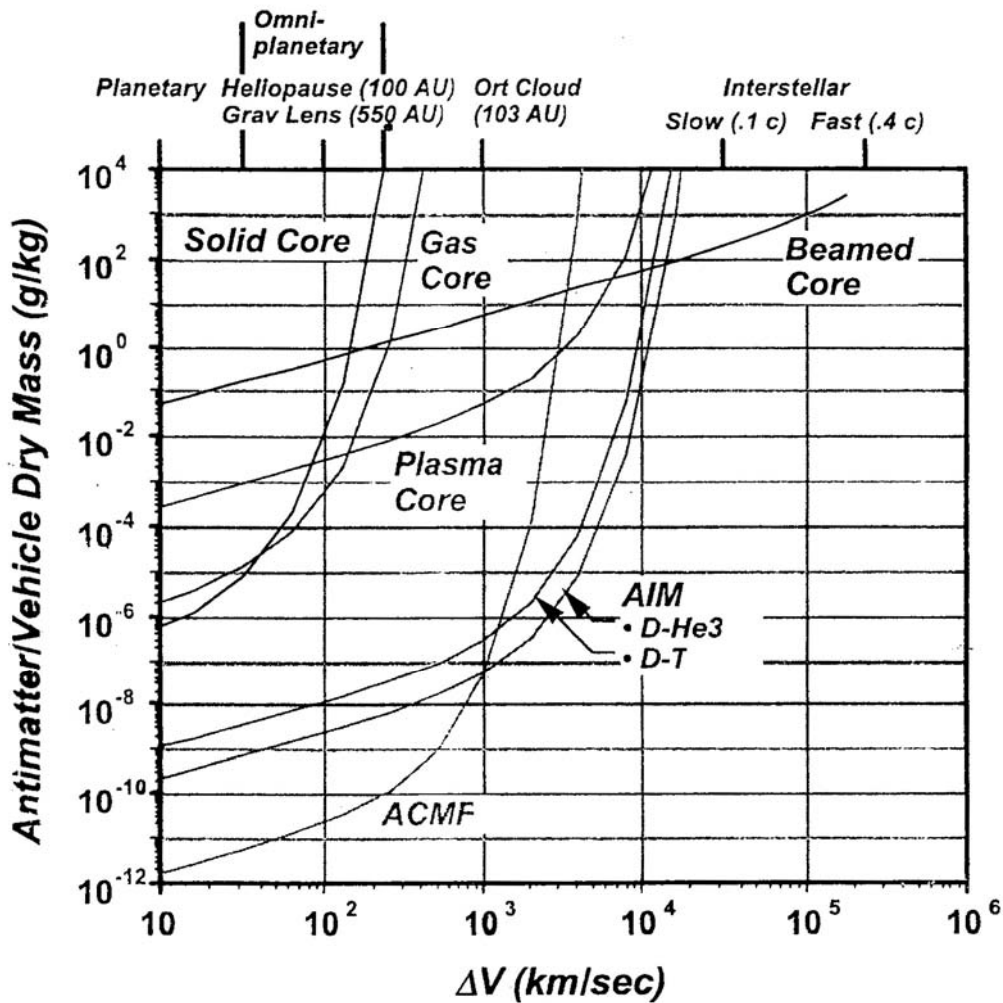


**Figure 21** - Antiproton mass requirements for various antimatter propulsion concepts

ACMF is clearly superior to all other concepts in terms of antimatter efficiency. This continues until we consider trips to Oort cloud and beyond. At this point the better performance with AIM overtakes ACMF and results in lower antimatter usage. ACMF's requirement is generally 2 orders of magnitude less for missions within the solar system.

## 6.4 - ANTIMATTER PRODUCTION AND STORAGE

### 6.4.1 - Antiproton manipulation

About 25 years ago, physicists at CERN began to seriously study ways to extend the capability of their existing accelerator in order to increase the proton collision energies of their high-energy particle experiments. They succeeded in doing this by incorporating an antiproton production capability into their main accelerator and by adding the Antiproton Collector (ACOL) for temporary storage. These upgrades enabled them to perform direct proton-antiproton collisions and effectively doubled the collision energies of their experiments. Soon thereafter, FNAL (Fermilab) built the Antiproton Accumulator (AA), a copy of CERN's ACOL. Today, the AA is at the center of FNAL's program involving  $1 \text{ TeV} \times 1 \text{ TeV}$  ( $1 \text{ TeV} = 10^{12}$  electron volts) collisions between antiprotons and protons.

In the early 1980's, CERN constructed the Low Energy Antiproton Ring (LEAR), an electromagnetic storage device which decelerates and cools antiprotons from the ACOL down to an energy of 5.9 MeV. Using LEAR as a supply, high intensity antiproton beams of extremely low emittance and energy resolution could be produced and made available for research in low-energy nuclear, particle and atomic physics. To free up funds for the Large Hadron Collider (LHC), CERN closed down LEAR at the end of 1996. However, many physicists successfully persuaded CERN to keep the ACOL running in a modified form called the Antiproton Decelerator (AD). The AD has all the beam characteristics of LEAR. However, instead of a continuous beam, it delivers 250 nanosecond bunches of  $10^7$  antiprotons every minute, which are ideal for collection and storage experiments using Penning traps and even more advanced devices.

The AD started operation in early-1999, and it is used primarily to support research aimed at studying the formation and spectroscopy of atomic antihydrogen. The long-term significance of this work is potentially enormous, since the ultimate, most efficient way of transporting antimatter to space could be in the form of electrically neutral atomic antihydrogen stored in miniature magnetic bottles. In the meantime, there will be many opportunities to carry out research with Penning-type traps filled with antiprotons at the AD. Assuming continuous operation, this device will be capable of producing  $10^{12}$  to  $10^{13}$  antiprotons per year which translates from 1.5 to 15 picograms ( $1.5 \times 10^{-12}$  to  $15 \times 10^{-12}$  grams).

In summary, antiprotons are currently produced in relatively small quantities, i.e., roughly 1 nanogram per year. Systems for deceleration and storage are available at CERN for important experiments in formation of antihydrogen atoms, and similar devices could become available at FNAL.

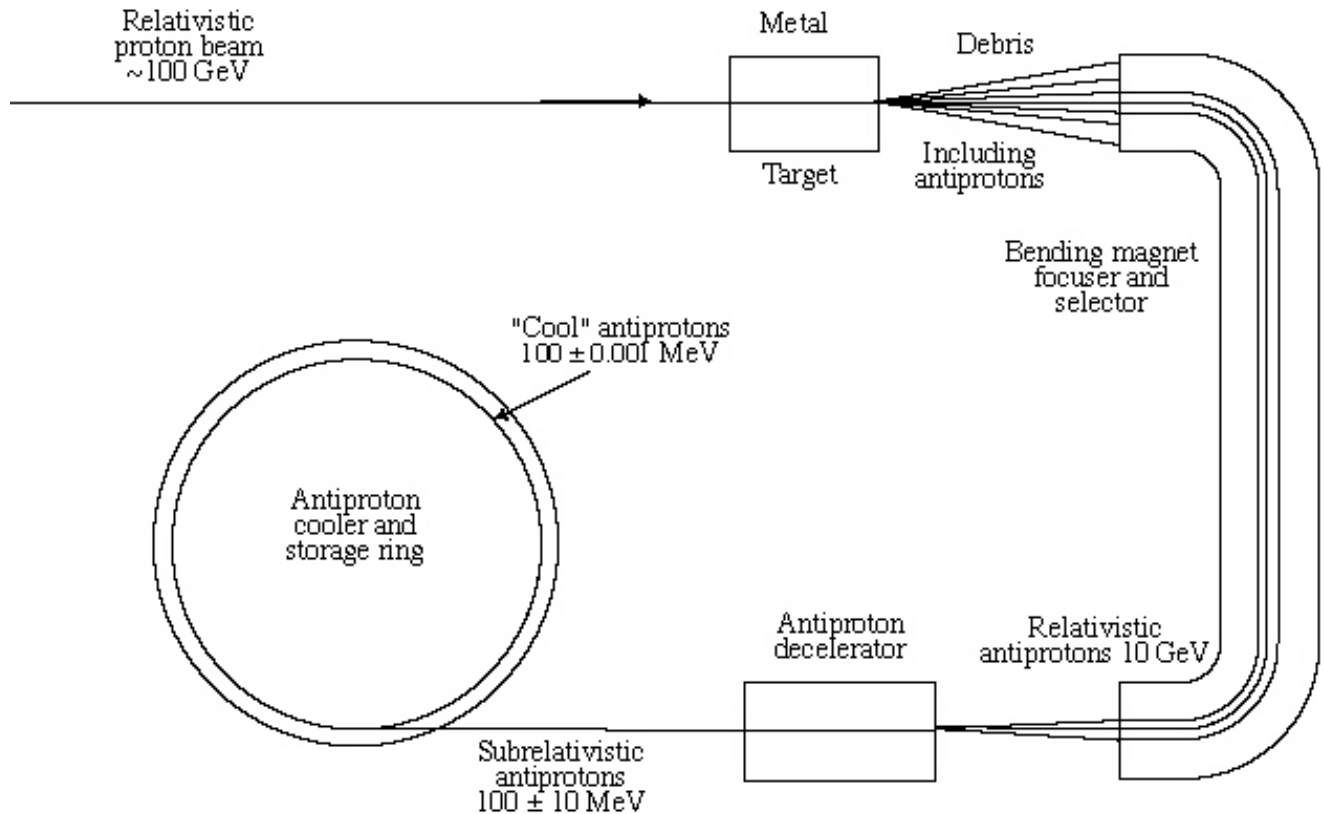
Antiprotons sources exist worldwide at two sources, CERN in Geneva, Switzerland and Fermilab, in Batavia, Illinois. These two laboratories utilize high energy proton synchrotron accelerators, with accumulator storage rings attached to collect antiprotons produced by collisions of protons on targets (Fig. 22). Presently, Fermilab collects  $6 \times 10^{10}$  antiprotons per hour in its Accumulator. This means that in one year of dedicated production, it could produce a maximum of 0.85 ng of antiprotons. A new and funded facility, called the Main Injector will turn on, with a maximum annual production capacity of 14 ng. A new Recycler Ring presently under construction and located inside the Main Injector ring will increase the collection rate by another factor of 10. This would place Fermilab in the 100 ng range, making it attractive for future space applications.

Final slowing down of antiproton beams could be achieved with the aid of a chirped laser frequency (Fig. 23).

Final trapping work can also be achieved through purely electromagnetic processing.

At CERN, the 5.9 MeV  $\bar{p}$  beam is degraded down to 10-30 keV and injected into a large Penning trap. The antiprotons are trapped radially by the magnetic field, and axially by the two confining electrostatic potentials. The harmonic frequencies of these two motions are around 50 and 5 MHz respectively. A third harmonic "magnetron" motion is also present. This precession around the direction of the  $\underline{E} \times \underline{B}$  vector is at a rate of about 80 kHz. Measurement of the actual number of antiprotons trapped is done by lowering the potential of the far electrode, allowing the antiprotons to spill out of the trap and annihilate into charged pions. Observed linear correlations between the

number of pion counts and the number of antiprotons injected into the trap show that at least  $10^6$  antiprotons per injection shot from LEAR have been trapped.



## Producing, capturing, and storing antiprotons

**Figure 22** - Producing, capturing, and storing antiprotons

Electrons cooling then permits collection of successive shots from LEAR, for example 10 successive shots would yield  $10^7$  antiprotons in the trap. Electron cooling is done by injecting electrons into the trap, where by collisions they absorb energy from the antiprotons. This energy is released by the electrons as they spin around the magnetic field in the form of synchrotron radiation. The data demonstrate lifetimes of up to several hours, corresponding to vacua of less than  $10^{-11}$  Torr.

### 6.4.2 - Transporting Antiprotons to Space

For space propulsion applications, 140 ng of antiprotons corresponds to about  $10^{17}$  antiprotons. One possible scenario therefore would be to transport  $10^3$  traps into space, each holding  $10^{14}$  antiprotons. It is likely that these  $10^3$  traps would be integrated into a common cryogenic system. Scale-up from traps holding  $10^7$  antiprotons to  $10^{14}$  antiprotons will not be trivial. Traps presently in use have a Brillouin limit of about  $10^{11}$  antiprotons/cc. Therefore, a trap with a volume of 1 liter can hold the required number of antiprotons.

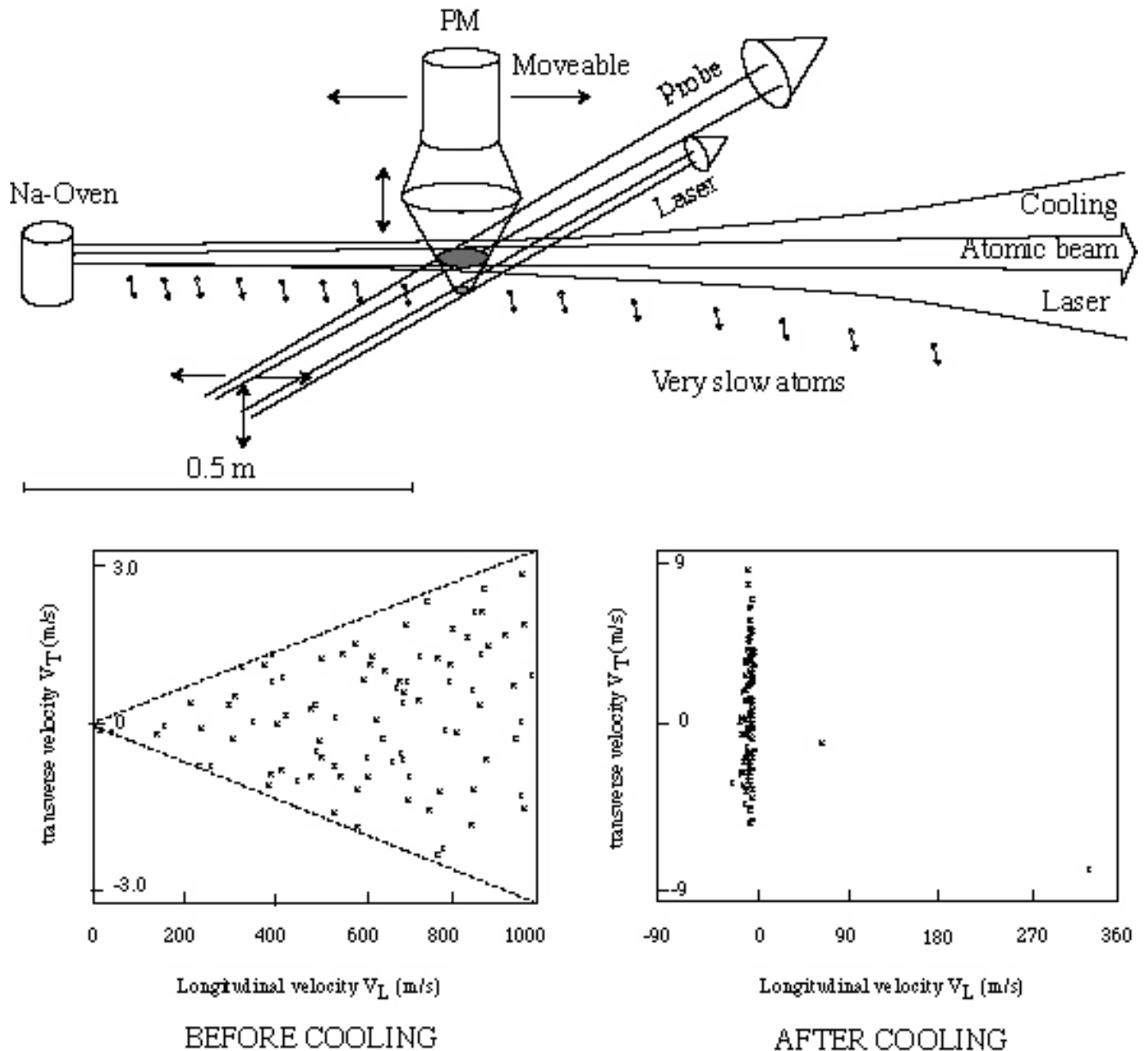


**Figure 23** - Particle slowing using chirped laser frequency

The Penn State Group [20] is presently building a portable antiproton trap. It is designed to carry up to  $10^9$  antiprotons for 4-10 days. It is a prototype for a trap capable of carrying  $10^{14}$  antiprotons for up to 120 days (duration of a round trip mission to Mars). The portable trap is one meter tall, 30 cm across, and weighs 125 kg. It operates at 4K temperature, supported by cryogenic nitrogen and helium reservoirs, and has a unique feature that the confining magnet is made of permanently magnetic SmCo materials, which should prove to be robust.

Test results to date are very encouraging. Up to 40 million electrons have been trapped for sixteen hours.  $H_2$  gas ( $\sim 1 \mu\text{mole}$ ) has been injected and the electron gun turned on. Bombardment of the gas by the electrons produces various charged ion species, including small numbers of  $H^+$  ions. The storage lifetime has been measured by extraction into a channeltron detector. Lifetimes of up to  $10^3$

seconds have been observed. The electron and  $H^+$  lifetime results are consistent with a vacuum in the inner trap of  $10^{-10}$  Torr.

Instabilities set in when the charged antiproton Coulomb energy density exceeds the magnetic (Penning trap) energy densities. Since there are practical limits to fields that can be supported, the next is to prepare accumulations of large numbers of antiprotons in the form of electrically neutral atoms, such as atomic antihydrogen. Within the fast years these atoms have been synthesized at CERN by injecting positronium atoms, bound electron-positron pairs, into a trap filled with antiprotons.

Those sparkling achievements are respectively due to the ATRAP (Gabrielse *et al.* [27]) collaboration and the ATHENA collaboration (Hangst *et al.* [28]). Then, one can try to produce and confine thousands of antihydrogen atoms in a Pritchard-Ioffe trap, consisting of a vacuum cylinder within a quadrupole magnet, augmented with confining pinch coils at each. Confinement is provided by the interaction of the atomic magnetic moment with the inhomogeneous magnetic field. This technology is currently available from laboratories studying atomic hydrogen where densities of  $> 10^{14}$  atoms/cc have been achieved. Although these densities are much higher than allowed by Penning traps, instabilities exist which prohibit their use at high densities for long term accumulation. The next step therefore involves forming condensates of electrically neutral molecular antihydrogen, either in liquid or solid form, which would provide densities approaching  $10^{23}$  atoms/cc; 140 ng of antihydrogen would constitute a spherical volume of about 60  $\mu\text{m}$  radius.

We assume that antihydrogen behaves exactly as hydrogen.

The techniques for trapping parahydrogen gas and the subsequent formation of solid parahydrogen may turn out to be relatively simple, or they may require complex ultrahigh vacuum chambers with many ports and windows, high-power lasers, and heavy electric or magnetic field generators. Once the small microcrystals or larger ice balls of parahydrogen ice are formed, however, they can be transferred to a compact electric traps for levitation.

The magnetic susceptibility of solid hydrogen depends upon its state. The orthohydrogen form has both of the protons in its nucleus with their magnetic moments pointing in the same direction, so it has a positive magnetic moment. The parahydrogen form has its two protons and its two electrons with their spins oriented in opposite directions so the particle spins cancel out. The only magnetic susceptibility left comes from the "currents" caused by orbital motion of the electrons around the nucleus.

The steps leading from  $\bar{p}$  beam to antihydrogen ice are detailed on Fig. 24.

Antihydrogen ice may then be [1] electrostatically levitated (Fig. 25). The ice particles need to be slightly charged, either positive or negative. This can be accomplished either by charging the ice positive by addition of extra the positrons or charging it negative by annihilating some of the positrons with electrons from an electron gun or driving off the positrons with ultraviolet light.

The well known Earnshaw Theorem states: "A charged body placed in an electric field of force cannot rest in stable equilibrium under the influence of the electric forces alone". This means that an electric levitation system has to have an active means of maintaining sufficient charge on the antihydrogen ice particles, as well as an active position control loop to maintain the particles in the center of the trap.

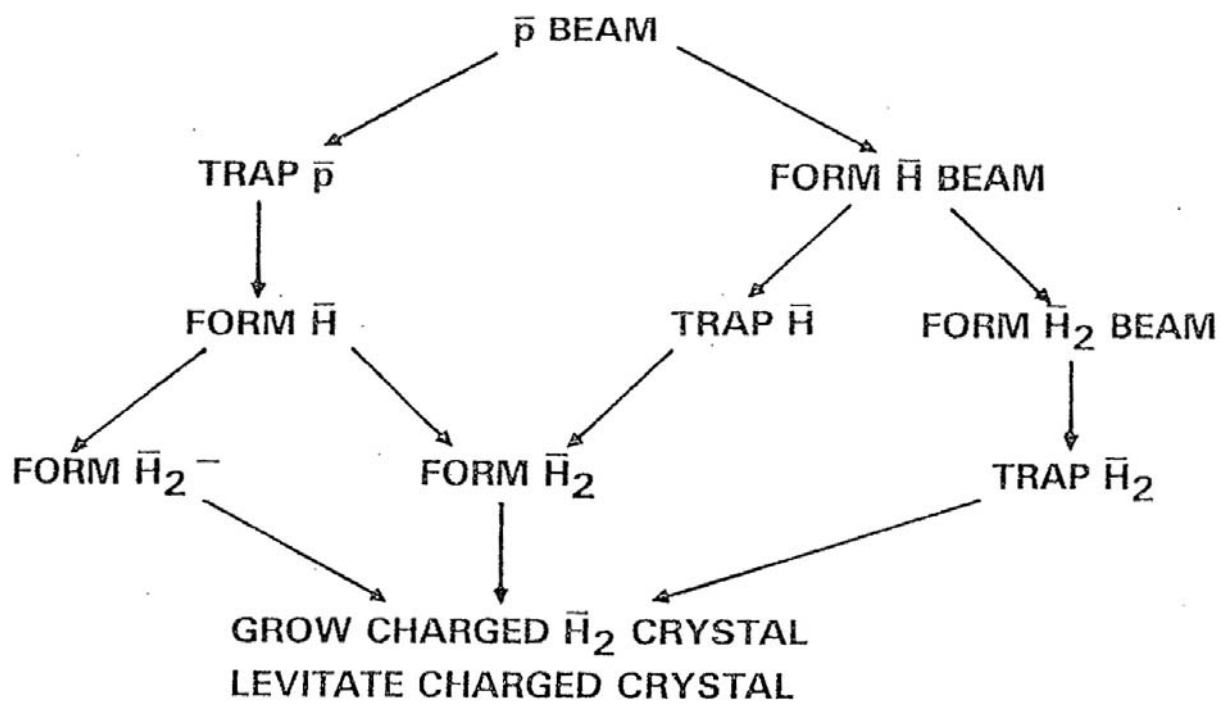


Figure 24 - Many paths from antiprotons to antihydrogen ice [1]

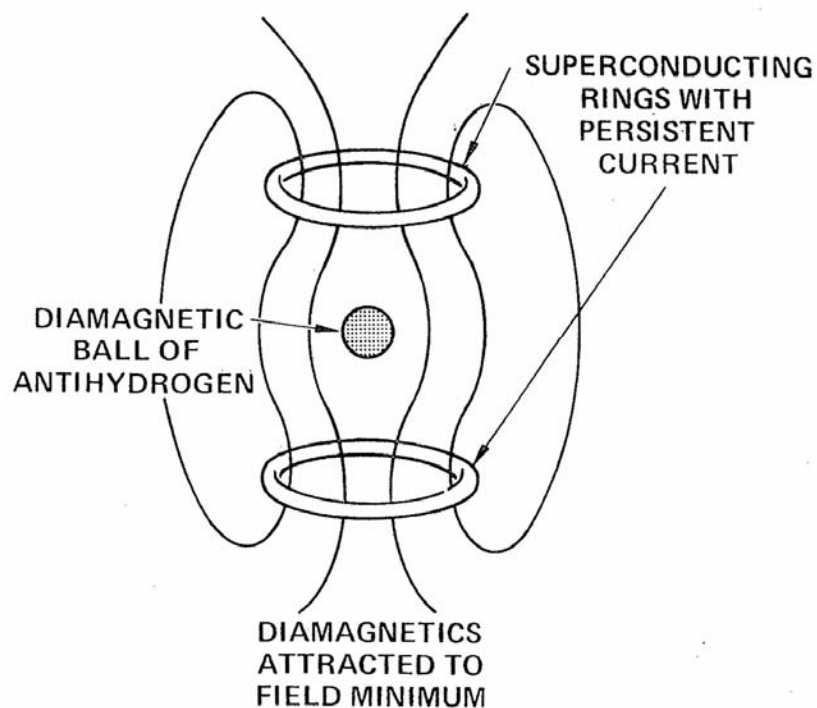


Figure 25 - Magnetostatic trap for antiparahydrogen ice

Serious technical issues include annihilation of surface atoms with residual gas in the confining vessel, and sublimation of surface atoms with resultant annihilation on the walls of the confining vessel. In the latter case, the annihilation could eject matter from the walls, which in turn annihilated with the antihydrogen, starting a chain reaction [29].

## 7 - SUMMARY

We have demonstrated the enormous potentialities afforded by thermonuclear fusion to the future of space propulsion throughout the whole solar system.

A decisive and first step beyond SCP might well be afforded by a clean combustion of fission,  $\bar{p}$ -annihilation with inertial compression of DT or D- $^3\text{He}$  fuel.

However, the slow albeit continuous progresses achieved by MFE and ICF could open the door to many more productive scenarios.

We did not discuss costs per se, because those would have been framed very differently for space propulsion than for energy production on earth. It should also be recalled that when thermonuclear energy is affordable, the cost of electricity might well be dropping by several orders of magnitude. So, even  $p$ - $\bar{p}$  annihilation could prove economically practical in a distant future.

It is now widely accepted that present technology could permit to envision ambitious robotic and manned exploration of the solar system, precursor interstellar study of phenomena outside the solar system, and missions to our closest stellar neighbors. These reflect the data used in a recent evaluation of propulsion options for interstellar missions [25]. The missions and their associated  $\Delta V$ 's are shown in Table IX.

A final optimistic touch arises from the steadily increasing antiproton production displayed on Fig. 26.

Table IX - Reference Missions

Mission	Description	Typical $\Delta V$ (km/s)
Planetary	Deep space robotic missions throughout solar system	10
Omniplanetary	Ambitious human exploration throughout solar system	30-200
100 - 1000 AU	Interstellar precursor mission to <ul style="list-style-type: none"> <li>• Heliopause (100 AU)</li> <li>• Gravity Lens focus (550 AU)</li> </ul>	100
10,000 AU	Interstellar precursor missions to Oort Cloud (10,000 AU)	1,000
Slow Interstellar	4.5 light-years in 40 years	30,000 (=0.1 c)
Fast Interstellar	4.5 light-years in 10 years or 40 light-years in 100 years	120,000 (=0.4 c)

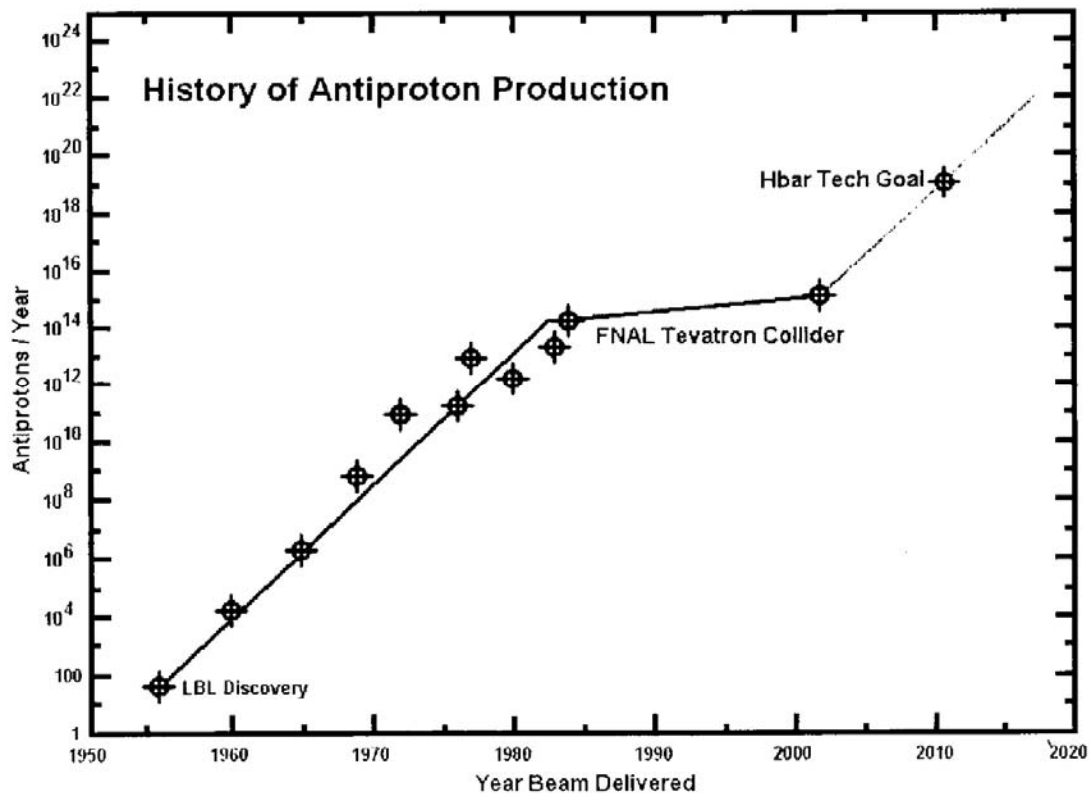


Figure 26 - Antiproton Production History

## BIBLIOGRAPHY

- [1] R.I. Forward, Antimatter Annihilation Propulsion, Air Force Rocket Propulsion Laboratory, Report AD-A160-734, Sept. 1985.
- [2] E. Teller, A.J. Glass, T.K. Fowler, A. Hasegawa and J.F. Santarius, Space propulsion by fusion in a magnetic dipole, *Fusion Technology*, **22**, 82 (1992).
- [3] J. Reece Roth, Space applications of fusion energy, *Fusion Technology*, **15**, 1375 (1989).
- [4] L.J. Wittenberg, J.F. Santarius and G. Kulcinski, Lunar Source of He-3 for commercial fusion power, *Fusion Technology* **10**, 167 (1986).
- [5] E. Stuhlinger, Ion propulsion for space flight, 1964, McGraw-Hill, New York.
- [6] F. Winterberg, On attainability of fusion temperatures under high densities by impact shock waves of small solid particles, *Zeits. Naturforsch* **19a**, 231 (1964).
- [7] C. Deutsch, Inertial confinement driven fusion by intense ion beams, *Ann-Phys. (Paris)* **11**, 1 (1986).



- [8] H. Ganswindt, Das jüngste Gerich, 1899 Berlin, Library of Congress, Catalogue No. TL 544, G3, 1899.
- [9] F. Winterberg, Possibility of producing a dense thermonuclear plasma by an intense field emission, *Phys. Rev.* **174**, 212 (1968).
- [10] C. Deutsch, Fast ignition schemes for inertial confinement fusion, *Eur. Phys. J. Appl. Phys.*, **24**, 95 (2003).
- [11] F. Winterberg, Rocket propulsion by staged thermonuclear explosions, *JBIS*, **30**, 333 (1977).
- [12] F. Winterberg, Ignition by shock-wave focussing and staggering of thermonuclear explosions, *Nature*, **258**, 512 (1975).
- [13] J. Nuckolls, A. Thiessen, L. Wood and G. Zimmermann, Laser compression of matter to super high densities, *Nature*, **239**, 139 (1972)
- [14] M.L. Shmatov, Space propulsion systems using ignition of microexplosion by distant microexplosions, *JBIS*, **53**, 62 (2000).
- [15] G.R. Schmidt, H.P. Gerrish and J.J. Martin, G.A. Smith and K.J. Meyer, Antimatter production for near-term propulsion applications, 1999, Joint Propulsion Conference.
- [16] G.A. Smith *et al.*, Antiproton production and trapping for space propulsion applications, Unpublished paper, available on-line.
- [17] R.L. Forward, Antiproton annihilation propulsion, *J. Propulsion*, **1**, 370 (1985).
- [18] G.A. Smith, G. Gaidos, R.A. Lewis and T. Schmidt, Aimstar: Antimatter initiated microfusion for precursor interstellar missions, *Acta Astronautica*, **44**, 183 (1999).
- [19] F.J. Dyson, Interstellar Transport, *Physics Today*, **21**, 41 (1968).
- [20] G. Gaidos, R.A. Lewis, G.A. Smith, B. Dundore and S. Chakrabarti, Antiproton-Catalyzed Microfission/Fusion Propulsion Systems for Exploration of the Outer Solar System and Beyond, *AIAA* **98-3589**, July 1998.
- [21] S.D. Howe and G.P. Jackson, Antimatter driven Sail for deep space exploration, 2004, [www.hbartech.com](http://www.hbartech.com)
- [22] S.D. Howe and J.D. Metzger, Antiproton-Based Propulsion Concepts and the Potential Impacts on a Manned Mars Mission, *J. Propulsion and Power*, **5**, 3 (1989).

- [23] S.K. Borowski, Comparison of Fusion/Antiproton Propulsion System for Interplanetary Travel, Fusion Energy in Space Propulsion, *AIAA Progress in Astronautics and Aeronautics*, Vol. **167**, 1995, Kammash, T. ed.
- [24] B.N. Cassenti, High Specific Impulse Antimatter Rockets, *AIAA* **91-2548**, June 1991.
- [25] R.H. Frisbee and S.D. Leifer, Evaluation of Propulsion Options for Interstellar Missions, *AIAA* **99-3403**, July 1998.
- [26] G. Gaidos, R.A. Lewis, K. Meyer, T. Schmidt and G.A. Smith, AIMStar Antimatter Initiated Microfusion for Precursor Interstellar Missions, *AIAA* **98-3404**, July 1998.
- [27] G. Gabrielse *et al.*, Driven Production of cold antihydrogen and the first measured distribution of antihydrogen states (A trap collaboration). *Phys. Rev. Lett.*, **89**, 233401 (2002).
- [28] J.S. Hangst *et al.*, Production and detection of cold antihydrogen atoms (Athena Collaboration), *Nature*, **419**, 456 (2002).
- [29] M.L. Shmatov, Some safety problems in the storage of solid antihydrogen, *Tech. Phys. Lett.*, **20**, 357 (1994).